

# The Search for Supersymmetry at the Tevatron Collider

M. Carena,<sup>1</sup> R.L. Culbertson,<sup>2</sup> S. Eno,<sup>3</sup> H.J. Frisch,<sup>2</sup> and S. Mrenna<sup>4</sup>

<sup>1</sup> *Fermi National Accelerator Laboratory*

<sup>2</sup> *University of Chicago*

<sup>3</sup> *University of Maryland*

<sup>4</sup> *Argonne National Laboratory*

## Abstract

We review the status of searches for Supersymmetry at the Tevatron Collider. After discussing the theoretical aspects relevant to the production and decay of supersymmetric particles at the Tevatron, we present the current results for Runs Ia and Ib as of the summer of 1997.

## 1 Introduction

The Tevatron is a  $p\bar{p}$  collider located at the Fermi National Accelerator Laboratory (Fermilab) in Batavia, Illinois, USA. Two experimental collaborations, CDF and DØ, have collected data at a  $p\bar{p}$  center-of-mass energy of  $\sqrt{s} = 1.8$  TeV. The CDF detector<sup>1</sup> features a magnetic solenoidal spectrometer inside the calorimeters and a silicon vertex detector; the DØ detector's<sup>2</sup> strengths are the finely-segmented hermetic calorimeter and the good muon coverage. There have been two major runs of the Tevatron, accumulating approximately 20 pb<sup>-1</sup> of data in '92-'93 and 100 pb<sup>-1</sup> in '94-'95. The next run, starting around 2000, will provide 1000 pb<sup>-1</sup> per year. Table 1 summarizes those CDF and DØ analyses that have been published or presented at conferences. This review addresses all analyses available as of summer 1997. Due to limited space here many details must be left out; a more thorough review is available including lists of cuts for each analysis and the basic theoretical tools necessary to understand the current and potential Tevatron analyses.<sup>3</sup>

The Tevatron Collider has been the world's accelerator-based high energy frontier since it first began taking data in 1987, and has thus been a prime location to search for the final pieces of the Standard Model (SM) and new phenomena beyond. Supersymmetry (SUSY)<sup>4</sup> is a new symmetry which provides a well-motivated extension of the SM. If SUSY is a consistent description of Nature, then the lower range of SUSY particle masses can be within the reach of the Tevatron, motivating a wide range of searches in a large number of channels.<sup>5</sup> The mass of the lightest neutral Higgs boson is strongly constrained within SUSY,<sup>6</sup> and could be within the reach of the upgraded Tevatron.<sup>7,8</sup>

## 2 The MSSM

In the past two decades, a detailed picture of the Minimal Supersymmetric extension of the Standard Model (MSSM), has emerged.<sup>9</sup> The details are discussed in other chapters of this book. In short, the MSSM contains the known SM particles plus SUSY partners: neutralinos  $\tilde{\chi}_{1-4}^0$ , charginos  $\tilde{\chi}_{1-2}^\pm$ , gluinos  $\tilde{g}$ , squarks  $\tilde{Q}_L$  and  $\tilde{Q}_R$ , sleptons  $\tilde{\ell}_L$  and  $\tilde{\ell}_R$ , sneutrinos  $\tilde{\nu}$ , and 3 neutral Higgses  $h, H$  and  $A$ , plus the charged Higgs  $H^\pm$ . In addition to the usual SM parameters, the masses and interactions of the sparticles depend on  $\tan\beta$ ,<sup>a</sup> the Higgsino mass parameter  $\mu$ ,<sup>b</sup> and a number of soft SUSY-breaking (SUSY) mass parameters which are added explicitly to the Lagrangian.

**Sparticle Spectrum:** The  $\tilde{\chi}_{1-2}^\pm$  and  $\tilde{\chi}_{1-4}^0$  masses and their gaugino and Higgsino composition are determined by  $M_W$ ,  $M_Z$ ,  $\tan\beta$ ,  $\mu$ , and two gaugino soft SUSY parameters  $M_1$  and  $M_2$ , all evaluated at the electroweak scale  $M_{EW}$ .<sup>c</sup> The  $\tilde{g}$  mass is determined by the  $SU(3)_C$  gaugino mass parameter  $M_3$ . Depending on the gaugino/Higgsinos composition, the  $\tilde{\chi}$  couplings to gauge bosons, and to  $L$  and  $R$  sfermions can differ substantially, strongly affecting production and decay processes.

The mass eigenstates of sfermions are, in principle, mixtures of their  $L$  and  $R$  components, and the magnitude of mixing is proportional to the mass of the corresponding fermion. The  $L - R$  mixing of  $\tilde{u}$ ,  $\tilde{d}$ ,  $\tilde{c}$ ,  $\tilde{s}$ ,  $\tilde{e}$  and  $\tilde{\mu}$  is thus negligible, and the  $L$  and  $R$  components are the real mass eigenstates, with masses  $m_{\tilde{Q}_{L,R}}$  and  $m_{\tilde{\ell}_{L,R}}, m_{\tilde{\nu}_\ell}$  fixed by soft SUSY parameters. For  $\tilde{t}$ ,  $\tilde{b}$  and  $\tilde{\tau}$ , the  $L - R$  mixing can be nontrivial. For example, the  $\tilde{t}$  mixing term is  $m_t(A_t - \mu/\tan\beta)$ , where  $A_t$  is a soft SUSY parameter.<sup>b</sup> Unless there is a cancellation between  $A_t$  and  $\mu/\tan\beta$ ,  $\tilde{t}$  mixing occurs because  $m_t$  is large, and it is possible that the lightest stop  $\tilde{t}_1$  is one of the lightest sparticles. For the  $\tilde{b}$  and  $\tilde{\tau}$ ,  $L - R$  mixing becomes important when  $m_b \tan\beta$  or  $m_\tau \tan\beta$  is  $\mathcal{O}(m_t)$ , since the  $\tilde{b}$  mixing term, for example, is  $m_b(A_b - \mu \tan\beta)$ .

At tree level, the lightest CP-even Higgs boson satisfies the relation  $M_h \lesssim M_Z$ , but this result is strongly modified by radiative corrections that depend on other MSSM parameters.<sup>12</sup> The dominant radiative corrections to  $M_h$  grow as  $m_t^4$  and are logarithmically dependent on the  $\tilde{t}$  and  $\tilde{b}$  masses. Within the MSSM, a *general upper* bound on  $M_h$  can be determined by a careful

<sup>a</sup>One Higgs doublet,  $H_2$ , couples to  $u, c$ , and  $t$ , while the other,  $H_1$ , couples to  $d, s, b, e, \mu$ , and  $\tau$ . The parameter  $\tan\beta$  is the ratio of vacuum expectation values  $\langle H_2 \rangle / \langle H_1 \rangle \equiv v_2 / v_1$ , and  $v^2 = v_1^2 + v_2^2$ , where  $v$  is the order parameter of EWSB  $\simeq 246$  GeV.

<sup>b</sup>Beware of different sign conventions for  $\mu$  and  $A_f$  in the literature. Both PYTHIA<sup>10</sup> and ISAJET<sup>11</sup> use the convention stated in S.P. Martin's review in this book.

<sup>c</sup>The electroweak scale  $M_{EW}$  is roughly the scale of the sparticle masses themselves. Usually, in the literature, for simplicity,  $M_{EW} \simeq M_Z$ .

evaluation of the one-loop and dominant two-loop radiative corrections.<sup>6</sup> After setting the masses of all SUSY particles and  $M_A$  to values around 1 TeV, setting  $\tan\beta > 20$ , and varying the  $\tilde{t}$  mixing parameters to give the largest possible effect, the upper bound on  $M_h$  is maximized, yielding  $M_h \lesssim 130$  GeV for  $m_t = 175$  GeV. For more moderate values of the MSSM parameters, the upper bound on  $M_h$  becomes smaller. Given the general upper bound on  $M_h$  of about 130 GeV, the upgraded Tevatron has the potential to provide a crucial test of the MSSM.<sup>7,8</sup>

The SUSY spectrum can be sensitive to the exact range of  $\tan\beta$ .<sup>13</sup> The measured value  $m_t \simeq 175$  GeV defines a lower bound on  $\tan\beta$  of about 1.2, provided that the top  $t$  Yukawa coupling remains finite up to a scale of the order of  $10^{16}$  GeV. If, instead, the  $t$  Yukawa coupling should remain finite only up to scales of order of a TeV, values of  $\tan\beta$  as low as .5 would still be possible.<sup>d</sup> Similarly, if  $\tan\beta$  becomes too large, large values of the  $b$  Yukawa coupling are necessary to obtain values of  $m_b$  compatible with experiment. Generically, it can be shown that values of  $\tan\beta \geq 60$  are difficult to obtain if the MSSM is expected to remain a valid theory up to scales of order  $10^{16}$  GeV.

**Supergravity (SUGRA):** At present, the exact mechanism of SUSY is unknown. SUGRA models assume the existence of extra superfields (the so-called “hidden sector”) which couple to the MSSM particles only through gravitational-like interactions. These interactions are responsible for inducing the soft SUSY parameters. The number of possible parameters is over 100, but in the minimal SUGRA (mSUGRA) scenario, all scalars (Higgs bosons, sleptons, and squarks) are assumed to have a common squared-mass  $m_0^2$ , all gauginos (Bino, Wino, and gluino) have a common mass  $m_{1/2}$ , and all triple-scalar couplings have the value  $A_0$ , all at a scale of order  $M_{\text{Planck}}$  (or, approximately,  $M_{GUT}$ , the scale where the gauge couplings unify). After specifying  $\tan\beta$ , all that remains is to relate the values of the soft SUSY parameters specified at  $M_{GUT}$  to their values at  $M_{EW}$ . This is accomplished using renormalization group equations (RGE’s). Moreover,  $\mu$  is determined up to a sign by demanding the correct electroweak symmetry breaking (EWSB). Finally, the physical sparticle masses are determined as a function of the low energy values of the soft SUSY parameters, which can be written in terms of  $m_0$ ,  $m_{1/2}$ ,  $A_0$ ,  $\tan\beta$ , and  $\mu$ .<sup>14</sup>

The masses of the  $\tilde{g}$ ’s,  $\tilde{\chi}^\pm$ ’s and  $\tilde{\chi}^0$ ’s are strongly correlated. Once the RGE evolution is included,  $\mu$  tends to be larger than  $M_1$  and  $M_2$ , becoming the largest as  $\tan\beta \rightarrow 1$ . As a result,  $\tilde{\chi}_1^0$ ,  $\tilde{\chi}_2^0$  and  $\tilde{\chi}_1^\pm$  tend to be gaugino-like,

---

<sup>d</sup>This implies that a perturbative description of the MSSM would only be valid up to the weak scale, which is, of course, not a very interesting possibility.

and  $\tilde{\chi}_1^0$  can be the LSP. The approximate mass hierarchy is  $M_{\tilde{\chi}_2^0} \simeq 2M_{\tilde{\chi}_1^0} \simeq M_{\tilde{\chi}_1^\pm} \simeq 1/3M_{\tilde{g}} \simeq 0.8m_{1/2}$ .<sup>e</sup>

Because  $\tilde{\ell}$ 's have only EW quantum numbers and the lepton Yukawa couplings are small, the  $\tilde{e}$  and  $\tilde{\mu}$  **SUSY** mass parameters do not evolve much from  $M_{GUT}$  to  $M_{EW}$  and are roughly given by  $m_{\tilde{\ell}_L}^2 \simeq m_0^2 + 0.5m_{1/2}^2$  and  $m_{\tilde{\ell}_R}^2 \simeq m_0^2 + 0.15m_{1/2}^2$ . The  $\tilde{\nu}$  mass is fixed by a sum rule  $m_{\tilde{\nu}_\ell}^2 = m_{\tilde{\ell}_L}^2 + M_W^2 \cos 2\beta$ , and, when  $m_0$  is small, the  $\tilde{\nu}$  can be the LSP instead of the  $\tilde{\chi}_1^0$ . For  $\tan \beta \geq 40$ , the  $\tilde{\tau}$  **SUSY** mass parameters also receive non-negligible contributions from the  $\tau$  Yukawa coupling.

The  $\tilde{Q}$  soft **SUSY** mass parameters evolve mainly through the strong coupling to the  $\tilde{g}$ , so their dependence on the common gaugino mass is stronger than for  $\tilde{\ell}$ 's. For  $\tilde{u}$ ,  $\tilde{d}$ ,  $\tilde{c}$  and  $\tilde{s}$ , the mass eigenstates are roughly given by  $m_{\tilde{Q}_L}^2 \simeq m_0^2 + 6.3m_{1/2}^2$  and  $m_{\tilde{Q}_R}^2 \simeq m_0^2 + 5.8m_{1/2}^2$ . The above relations between the mass parameters lead to the general SUGRA prediction,  $m_{\tilde{Q}} \geq 0.85M_{\tilde{g}}$ .

In general, the  $\tilde{Q}$ 's are heavier than the  $\tilde{\ell}$ 's or the lightest  $\tilde{\chi}^0$  and  $\tilde{\chi}^\pm$ . For the  $L$  and  $R$  components and the  $L - R$  mixing of  $\tilde{t}$  and  $\tilde{b}$  and for the Higgs soft **SUSY** parameters, the large  $t$  Yukawa coupling (and possibly the  $b$  Yukawa coupling for large  $\tan \beta$ ) plays a crucial role in the RGE evolution. As a result, the  $\tilde{t}$  and  $\tilde{b}$  can be light. In this case, the coefficients of  $m_0$  and  $m_{1/2}$  have an important dependence on the low-energy values of the  $b$  and  $t$  Yukawa couplings which, in turn, depend on  $\tan \beta$ .<sup>3</sup> The coefficients of  $m_{1/2}$  depend on the exact values of  $\alpha_s$  and the scale of the sparticle masses.

Although mSUGRA is defined in terms of only 5 parameters at a high scale ( $m_0$ ,  $m_{1/2}$ ,  $A_0$ ,  $\tan \beta$ , and the sign of  $\mu$ ), it is natural to question exact universality of the soft **SUSY** parameters.<sup>15</sup> For example, in a  $SU(5)$  **SUSY** GUT model, the  $\tilde{e}_L$  and  $\tilde{d}_R$  reside in the same 5-multiplet of  $SU(5)$ , and may naturally have the common mass parameter  $m_0^{(5)}$  at the GUT scale. Similarly,  $\tilde{u}_L$ ,  $\tilde{d}_L$ ,  $\tilde{u}_R$ , and  $\tilde{e}_R$ , which reside in the same 10-multiplet, may have a common mass  $m_0^{(10)}$ . The two Higgs bosons doublets reside in different 5- and  $\bar{5}$ -multiplets, with masses  $m_0^{(5')}$  and  $m_0^{(\bar{5})'}$ . There is no known symmetry principle that demands that all these mass parameters should be the same.

**Gauge-Mediated Supersymmetry Breaking:** In contrast to SUGRA, the soft **SUSY** terms in the MSSM Lagrangian, can be generated through gauge interactions at a scale much lower than  $M_{\text{Planck}}$ , introducing many in-

<sup>e</sup>In general, it may occur that  $m_{1/2} \simeq 0$ . Low-energy gaugino masses are then dominated by contributions of stop-top and Higgs-Higgsino loops. In this case the  $\tilde{g}$  could be the LSP with a mass of a few GeV, and the  $\tilde{\chi}_1^0$  may be somewhat heavier due to contributions from electroweak loops.<sup>16</sup>

interesting features. In most models of gauge-mediated, low-energy SUSY, the gaugino and scalar masses are roughly of the same order of magnitude. Even after RGE evolution, sfermions with the same quantum numbers acquire the same masses (ignoring the effects of Yukawa couplings), yielding a natural mass hierarchy between weakly and strongly interacting sfermions; the mass hierarchy of the gauginos is fixed by the gauge couplings (as in SUGRA models). One distinctive feature of these models is that the spin-3/2 superpartner of the graviton, the gravitino  $\tilde{G}$ , can be very light and become the LSP,<sup>f</sup> unlike in SUGRA models, where the gravitino has a mass on the order of the electroweak scale and is very weakly interacting.

**R-Parity Violation ( $\mathbf{\tilde{R}}$ ):** A multiplicative R-parity symmetry is often assumed, but one simple extension of the MSSM is to break it.<sup>19</sup> Presently, neither experiment nor any theoretical argument demands R-parity conservation. There are several effects on the SUSY phenomenology associated with  $\mathbf{\tilde{R}}$  couplings: (1) lepton or baryon number violating processes are allowed, including the production of single sparticles (instead of pair production), (2) the LSP is no longer stable, but might decay to SM particles within a collider detector, and (3) because it is unstable, the LSP need not be the  $\tilde{\chi}^0$  or  $\tilde{\nu}$ , but can be charged or colored. Although very strong bounds on  $\mathbf{\tilde{R}}$  operators can be derived from the present data,<sup>20</sup> but there is still room for study.

**Run Ia Parameter Sets (RIPS):** Some CDF and DØ SUSY searches are analyzed in the framework of so-called “SUGRA-inspired models.” These RIPS are specified by  $M_{\tilde{g}}, m_{\tilde{Q}}, M_A, \tan\beta$  and the magnitude and sign of  $\mu$ .  $M_{\tilde{g}}$  defines  $M_1$  and  $M_2$  using SUGRA unification relations. The  $\tilde{\chi}^\pm$  and  $\tilde{\chi}^0$  properties are then fixed by  $\tan\beta$  and  $\mu$ . In practice, the value of  $\mu$  is set much larger than  $M_1$  and  $M_2$ , so the properties of the  $\tilde{\chi}^0$ ’s,  $\tilde{\chi}^\pm$ ’s, and  $\tilde{g}$  are similar to those in a pure SUGRA model. The first 5 flavors of  $\tilde{Q}$ ’s are degenerate in mass, with the value  $m_{\tilde{Q}}$ , while the stop masses are  $m_{\tilde{t}_1} = m_{\tilde{t}_2} = \sqrt{m_{\tilde{Q}}^2 + m_t^2}$ , assuming also the absence of  $L-R$  mixing. This may be quite unrealistic, since the  $\tilde{b}$  and  $\tilde{t}$  mass can be naturally lighter. When  $m_{\tilde{Q}} > M_{\tilde{g}}$ , the  $\tilde{\ell}$  masses can be fixed using approximate SUGRA relations, and the RIPS has many features of a SUGRA model. The region  $m_{\tilde{Q}} < M_{\tilde{g}}$  is very hard to realize in SUGRA models, but is also worth investigating. In this case, for some analyses, a constant value of 350 GeV is used for  $m_{\tilde{\ell}_L}$ ,  $m_{\tilde{\ell}_R}$ , and  $m_{\tilde{\nu}}$ . Finally, the Higgs mass  $M_A$  is used to determine the Higgs boson sector. In practice,  $M_A$  is set to a large value, so that the lightest neutral Higgs boson  $h$  has SM-like couplings

---

<sup>f</sup>It is also possible to construct a model where the gluino is a stable LSP with a mass of a few tens of GeV.<sup>18</sup> In this case, the missing energy signal for SUSY disappears, since a stable LSP gluino will form stable hadrons.

to gauge bosons and fermions, and all other Higgs bosons are heavy.

### 3 The Present Status of Sparticle Searches

#### 3.1 Charginos and Neutralinos

$\tilde{\chi}^\pm$  and  $\tilde{\chi}^0$  pairs can be produced directly at hadron colliders through electroweak processes. The cross sections are functions of the sparticle masses and mixings, with different contributions from t-channel  $\tilde{Q}$  exchange, s-channel vector boson production, and t- and s-channel interference. Figure 1 shows the production cross sections of various  $\tilde{\chi}^\pm$  and  $\tilde{\chi}^0$  pairs at the Tevatron in the limits of large and small  $|\mu|$  relative to the soft **SUSY** masses  $M_1$  and  $M_2$ . The decay patterns also depend on the masses and mixings. Two-body decays dominate if allowed:  $\tilde{\chi}_i^\pm \rightarrow W^\pm \tilde{\chi}_j^0$ ,  $H^\pm \tilde{\chi}_j^0$ ,  $\tilde{\chi}_j^\pm h$ ,  $\tilde{\chi}_j^\pm Z$ ,  $\tilde{\ell}_{L,R} \nu$ ,  $\tilde{\nu} \ell$  or  $\tilde{Q} q'$  and  $\tilde{\chi}_i^0 \rightarrow Z \tilde{\chi}_j^0$ ,  $h \tilde{\chi}_j^0$ ,  $W^\mp \tilde{\chi}_j^\pm$ ,  $H^\mp \tilde{\chi}_j^\pm$ ,  $\tilde{\ell}_{L,R} \ell$ ,  $\tilde{\nu} \nu$ , or  $\tilde{Q} q$ . When no 2-body final states are kinematically allowed, 3-body decays like  $\tilde{\chi}_i^\pm \rightarrow \tilde{\chi}_j^0 f \bar{f}'$ ,  $\tilde{\chi}_i^\pm \rightarrow \tilde{\chi}_j^\pm f \bar{f}$ ,  $\tilde{\chi}_i^0 \rightarrow \tilde{\chi}_j^\pm f \bar{f}'$ , and  $\tilde{\chi}_i^0 \rightarrow \tilde{\chi}_j^0 f \bar{f}$  occur through virtual sfermions and gauge bosons. If the sparticles are light enough, a 100% branching ratio to  $\ell \nu$ ,  $\ell^+ \ell^-$  or  $j j$  final states is possible. The one-loop decay  $\tilde{\chi}_2^0 \rightarrow \tilde{\chi}_1^0 \gamma$  can be important if the  $\tilde{\chi}_1^0$  is Higgsino-like and  $\tilde{\chi}_2^0$  is gaugino-like, or *vice versa*. For a light enough  $\tilde{g}$ , the decays  $\tilde{\chi}_i^\pm \rightarrow \tilde{g} f \bar{f}'$  and  $\tilde{\chi}_i^0 \rightarrow \tilde{g} f \bar{f}$  can be important.

The production of  $\tilde{\chi}_1^\pm \tilde{\chi}_2^0$ , followed by the decays  $\tilde{\chi}_1^\pm \rightarrow \tilde{\chi}_1^0 \ell \nu$  and  $\tilde{\chi}_2^0 \rightarrow \ell^+ \ell^- \tilde{\chi}_1^0$ , is a source of three charged leptons ( $e$  or  $\mu$ ) and  $\cancel{E}_T$ . This trilepton signal has small SM backgrounds, and is consequently one of the “golden” SUSY signatures.<sup>21</sup>

The results of the CDF<sup>22,23</sup> and DØ searches<sup>24,25</sup> are shown in Fig. 2 analyzed using RIPS. The searches include 4 channels:  $e^+ e^- e^\pm$ ,  $e^+ e^- \mu^\pm$ ,  $e^\pm \mu^+ \mu^-$  and  $\mu^\pm \mu^+ \mu^-$ . The CDF analysis requires one lepton with  $E_T > 11$  GeV, passing tight identification cuts, and two other leptons with  $E_T > 5$  GeV ( $e$ ) or  $p_T > 4$  GeV ( $\mu$ ), passing loose identification cuts. All leptons must be isolated, meaning there is little excess  $E_T$  in a cone of size  $R = 0.4$  in  $\eta - \phi$  space centered on the lepton. The event must have two leptons with the same flavor and opposite sign. If two leptons of the same flavor and opposite charge have a mass consistent with the  $J/\Psi$ ,  $\Upsilon$  or  $Z$  boson, the event is rejected. After this selection, 6 events remain in the data set, while the expected background, dominated by Drell-Yan pair production plus a fake lepton, is 8 events. After demanding  $\cancel{E}_T > 15$  GeV, no events remain, while 1.2 are expected from SM model sources.

The DØ analysis requires 3 leptons with  $E_T > 5$  GeV. However, several different triggers are used, and some lepton categories are required to have a

Table 1: A compilation of results from Run I Tevatron SUSY searches as of the summer of 1997. The symbol  $b$  denotes an additional  $b$ -tagged jet. Also listed are the references and the section of this chapter where each analysis is discussed. More information is available for DØ at <http://www-d0.fnal.gov/public/new/new-public.html>, and for CDF at <http://www-cdf.fnal.gov/>

| Sparticle                       | Signature   | Expt. | Run | $\int \mathcal{L} dt (\text{pb}^{-1})$ | Ref. | Sec. |
|---------------------------------|---|-------|-----|--|------|------|
| Charginos<br>and<br>Neutralinos | $\cancel{E}_T + \text{trilepton}$                     | CDF   | Ia  | 19                                     | [22] | 3.1  |
|                                 | $\cancel{E}_T + \text{trilepton}$                     | CDF   | Iab | 107                                    | [23] | "    |
|                                 | $\cancel{E}_T + \text{trilepton}$                     | DØ    | Ia  | 12.5                                   | [24] | "    |
|                                 | $\cancel{E}_T + \text{trilepton}$                     | DØ    | Ib  | 95                                     | [25] | "    |
|                                 | $\gamma\gamma + \cancel{E}_T$ or jets                 | CDF   | Ib  | 85                                     | [74] | 4.7  |
|                                 | $\gamma\gamma + \cancel{E}_T$                         | DØ    | Iab | 106                                    | [75] | "    |
| Squarks<br>and<br>Gluinos       | $\cancel{E}_T + \geq 3, 4$ jets                       | CDF   | Ia  | 19                                     | [35] | 3.2  |
|                                 | $\cancel{E}_T + \geq 3, 4$ jets                       | DØ    | Ia  | 13.5                                   | [31] | "    |
|                                 | $\cancel{E}_T + \geq 3$ jets                          | DØ    | Ib  | 79.2                                   | [32] | "    |
|                                 | dilepton + $\geq 2$ jets                              | CDF   | Ia  | 19                                     | [37] | "    |
|                                 | $\cancel{E}_T + \text{dilepton} + \geq 2$ jets        | CDF   | Ib  | 81                                     | [38] | "    |
|                                 | $\cancel{E}_T + \text{dilepton}$                      | DØ    | Ib  | 92.9                                   | [36] | "    |
| Stop                            | $\cancel{E}_T + \ell + \geq 2$ jets + $b$             | CDF   | Ib  | 90                                     | [42] | "    |
|                                 | $\cancel{E}_T + \ell + \geq 3$ jets + $b$             | CDF   | Iab | 110                                    | [44] | "    |
|                                 | dilepton + jets                                       | DØ    | Ib  | 74.5                                   | [43] | "    |
|                                 | $\cancel{E}_T + 2$ jets                               | DØ    | Ia  | 7.4                                    | [41] | "    |
|                                 | $\cancel{E}_T + \gamma + b$                           | CDF   | Ib  | 85                                     | [74] | 4.11 |
| Sleptons                        | $\gamma\gamma \cancel{E}_T$                           | DØ    | Iab | 106                                    | [75] | 3.7  |
| Charged<br>Higgs                | dilepton + $\cancel{E}_T$                             | CDF   | Ia  | 19                                     | [57] | 3.4  |
|                                 | $\tau + 2$ jets + $\cancel{E}_T$                      | CDF   | Ia  | 19                                     | [56] | "    |
|                                 | $\tau + b + \cancel{E}_T + (\ell, \tau, \text{jet})$  | CDF   | Iab | 91                                     | [48] | "    |
|                                 | $\tau + b + \cancel{E}_T + (\ell, \tau, \text{jet})$  | DØ    | Iab | 125                                    | [49] | "    |
| Neutral<br>Higgs                | $WH \rightarrow \ell + \cancel{E}_T + b + \text{jet}$ | CDF   | Iab | 109                                    | [53] | 3.5  |
|                                 | $WH \rightarrow \ell + \cancel{E}_T + b + \text{jet}$ | DØ    | Ib  | 100                                    | [52] | "    |
|                                 | $WH, ZH \rightarrow \gamma\gamma + 2$ jets            | DØ    | Ib  | 101.2                                  | [55] | "    |
|                                 | $ZH \rightarrow b + \text{jet} + \cancel{E}_T$        | DØ    | Ib  | 20                                     | [58] | "    |
|                                 | $WH, ZH \rightarrow 2$ jets + $2$ $b$ 's              | CDF   | Ib  | 91                                     | [54] | "    |
| $R$ violating                   | dilepton + $\geq 2$ jets                              | CDF   | Iab | 105                                    | [61] | 3.6  |
| Charged LSP                     | slow, long-lived particle                             | CDF   | Ib  | 90                                     | [59] | 3.6  |

larger  $E_T$  to pass the various trigger thresholds. All leptons are required to be isolated. To reduce events with mismeasured  $\cancel{E}_T$ , the  $\cancel{E}_T$  direction must not be along or opposite to a muon. Additional cuts are tuned for each topology. For

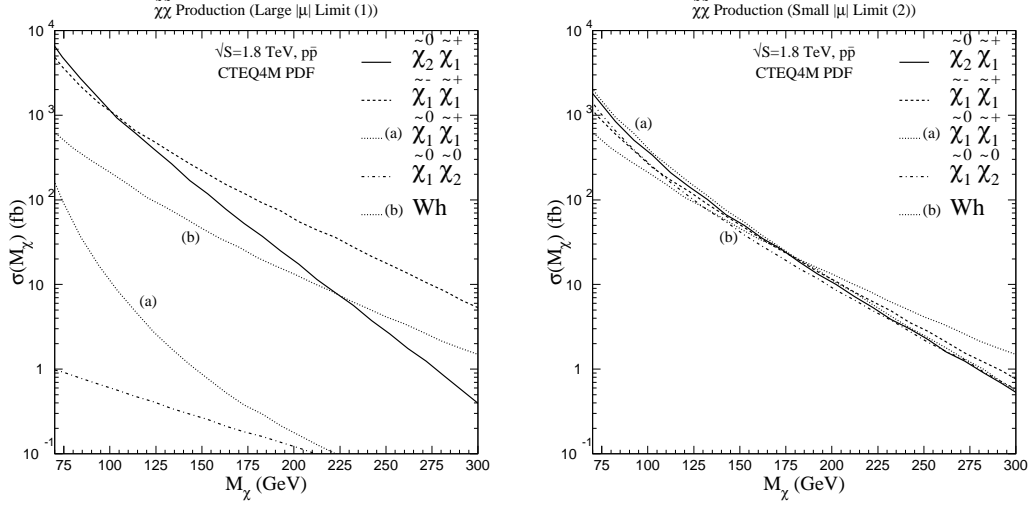


Figure 1: Production cross sections at the Tevatron for  $\tilde{\chi}_1^\pm$  and  $\tilde{\chi}^0$  pair production, assuming  $\tan \beta = 2$ ,  $m_{\tilde{Q}} = 500$  GeV, and  $M_1 = \frac{1}{2}M_2$ , versus the  $\tilde{\chi}_1^\pm$  mass. The left figure is generated by fixing  $\mu = -1$  TeV and varying  $m_{1/2}$ , the right figure by fixing  $m_{1/2} = 1$  TeV and varying  $\mu$ . The  $Wh$  cross section (curve  $b$ ) is shown for reference as a function of  $M_h$ .

example, the background from Drell–Yan pair production plus a fake lepton is highest in the  $eee$  channel, so these events are rejected if an electron pair is back-to-back. The  $\cancel{E}_T$  threshold is 15 GeV for  $eee$ , and 10 GeV for the other three topologies. No events are observed in any channel with a total of 1.26 events expected from (i) Drell–Yan production plus a fake lepton and (ii) heavy-flavor production.

The DØ limit is on the “average” of the 4 modes, while the CDF limit is on the sum. After accounting for this difference, the CDF limit is twice as sensitive at a given  $\tilde{\chi}_1^\pm$  mass. The CDF limit shown is compared to three RIPS, which have different ratios of  $m_{\tilde{Q}}$  to  $M_{\tilde{g}}$ . The DØ limit is compared to a wide variation of possible branching ratios. The DØ theory curve assumes heavy  $\tilde{Q}$ ’s, which reduces the cross section, but the CDF curves do not. The wide differences in the theory curves in Fig. 2 show the dangers of quoting a mass limit rather than a cross section  $\times$  branching ratio limit.<sup>27</sup>



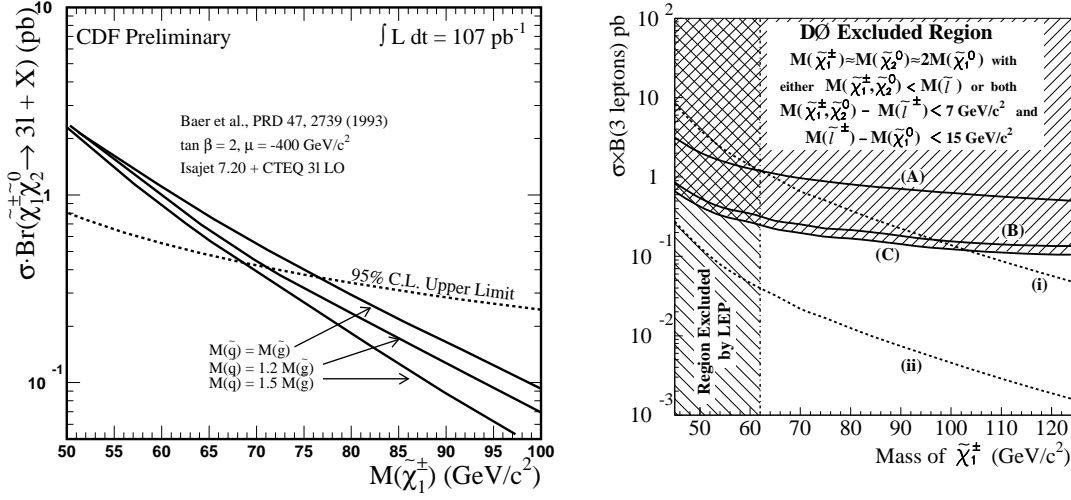


Figure 2: (Left) The CDF 95% C.L. limits on cross section  $\times$  branching ratio for  $\tilde{\chi}_1^{\pm} \tilde{\chi}_2^0$  production in  $107 \text{ pb}^{-1}$  of data. The limit is on the *sum* of the final states  $eee, ee\mu, \mu\mu\mu$  and  $\mu\mu e$  when  $\tilde{\chi}_1^{\pm} \rightarrow \ell\nu\tilde{\chi}_1^0$  and  $\tilde{\chi}_2^0 \rightarrow \ell\ell\tilde{\chi}_1^0$ . The signals expected for three different RIPS scenarios are shown for comparison.<sup>26</sup> (Right) Similar limits from DØ, but for the *average* of all four channels. The curves (A), (B), and (C) show the Run Ia, Run Ib, and combined limits. Curve (i) shows the predicted cross section  $\times$  branching ratio assuming  $\text{Br}(\tilde{\chi}_1^{\pm} \rightarrow \ell\nu\tilde{\chi}_1^0) = \text{Br}(\tilde{\chi}_2^0 \rightarrow \ell^+\ell^-\tilde{\chi}_1^0) = 1/3$  ( $\ell = e, \mu, \tau$ ). Curve (ii) assumes  $\text{Br}(\tilde{\chi}_1^{\pm} \rightarrow \ell\nu\tilde{\chi}_1^0) = 0.1$  and  $\text{Br}(\tilde{\chi}_2^0 \rightarrow \ell^+\ell^-\tilde{\chi}_1^0) = 0.033$ . For both CDF and DØ, kinematic efficiencies are calculated using the production cross section from ISAJET.

### 3.2 Squarks and Gluinos

The Tevatron is a hadron collider, so it can produce  $\tilde{g}$ 's and  $\tilde{Q}$ 's through their  $SU(3)_C$  couplings to quarks and gluons. The dominant production mechanisms are  $gg, q\bar{q} \rightarrow \tilde{g}\tilde{g}$  or  $\tilde{Q}\tilde{Q}^*$ ,  $q\bar{q} \rightarrow \tilde{Q}\tilde{Q}$  and  $qg \rightarrow \tilde{Q}\tilde{g}, \bar{q}g \rightarrow \tilde{Q}^*\tilde{g}$ , and the cross sections can be calculated as a function of only the  $\tilde{Q}$  and  $\tilde{g}$  masses (ignoring EW radiative corrections). Figure 3 shows the cross sections for  $\tilde{Q}$ 's and  $\tilde{g}$ 's as a function of the sparticle masses at  $\sqrt{s} = 1.8 \text{ TeV}$  (left) and  $2 \text{ TeV}$  (right), where NLO SUSY QCD corrections have been included.<sup>28</sup> The NLO corrections are in general significant, positive (evaluated at a scale equal to the average mass of the two produced particles), and much less sensitive to the choice of scale than a LO calculation.

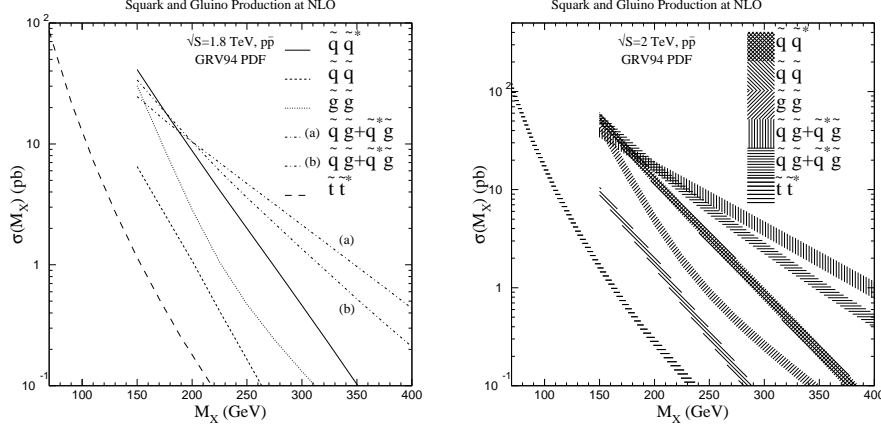


Figure 3: (Left) Production cross sections for  $\tilde{g}$ 's and  $\tilde{Q}$ 's versus sparticle mass  $M_X$  at the Tevatron,  $\sqrt{s} = 1.8$  TeV, assuming degenerate masses for 5 flavors of  $\tilde{Q}$ 's. For  $\tilde{Q}\tilde{Q}^*$  and  $\tilde{Q}\tilde{Q}$  production,  $M_X$  is the squark mass and  $M_{\tilde{g}} = 200$  GeV. For  $\tilde{g}\tilde{g}$  production,  $M_X$  is the  $\tilde{g}$  mass and  $M_{\tilde{Q}} = 200$  GeV. For  $\tilde{Q}\tilde{g}$  production (a),  $M_X$  is the  $\tilde{Q}$  mass and  $M_{\tilde{g}} = 200$  GeV; for (b),  $M_X$  is the  $\tilde{g}$  mass and  $M_{\tilde{Q}} = 200$  GeV. For  $t\bar{t}$  production,  $M_X$  is the stop mass. All cross sections are evaluated at a scale equal to the average mass of the two produced particles. (Right) The same curves with  $\sqrt{s} = 2$  TeV. The bands show the change in rate from varying the scale from 1/2 to 2 times the average mass of the produced particles.

Since  $\tilde{Q}$ 's and  $\tilde{g}$ 's decay into  $\tilde{\chi}^\pm$ 's and  $\tilde{\chi}^0$ 's, their signatures can be similar to  $\tilde{\chi}^\pm$  and  $\tilde{\chi}^0$  pair production, but with accompanying jets. If  $m_{\tilde{Q}} > M_{\tilde{g}}$ , then the  $\tilde{Q}$  has the 2-body decay  $\tilde{Q} \rightarrow \tilde{g}q$ . The  $\tilde{g}$  has then the possible decays  $\tilde{g} \rightarrow q\bar{q}\tilde{\chi}_i^\pm$  or  $\tilde{g} \rightarrow q\bar{q}'\tilde{\chi}_i^\pm$ , where  $q$  can stand for  $t$  or  $b$  as well, or even  $\tilde{g} \rightarrow t\bar{t}^*$  or  $t\bar{t}$  if kinematically allowed. The  $\tilde{g}$  can also decay at one-loop like  $\tilde{g} \rightarrow g\tilde{\chi}_i^0$ . If, instead,  $m_{\tilde{Q}} < M_{\tilde{g}}$ , then the  $\tilde{g}$  has the 2-body decay  $\tilde{g} \rightarrow \tilde{Q}q$ . The  $\tilde{Q}$ 's can then decay as  $\tilde{Q}_{L,R} \rightarrow q\tilde{\chi}_i^0$ ,  $\tilde{u}_L \rightarrow d\tilde{\chi}_i^+$ , and  $\tilde{d}_L \rightarrow u\tilde{\chi}_i^-$ . The  $\tilde{g}$ 's and  $\tilde{Q}$ 's may also be produced in association with  $\tilde{\chi}^\pm$ 's or  $\tilde{\chi}^0$ 's (analogous to  $W + j$  and  $Z + j$  production). Event signatures are similar to  $\tilde{Q}$  and  $\tilde{g}$  production, but possibly with fewer jets. Promising signatures for  $\tilde{Q}$  and  $\tilde{g}$  production are (i) multiple jets and  $\cancel{E}_T$ <sup>29</sup> and (ii) isolated leptons and jets and  $\cancel{E}_T$ .<sup>30</sup>

**Jets +  $\cancel{E}_T$ :** Both CDF and DØ have performed searches for events with jets and  $\cancel{E}_T$ . This signature has significant physics and instrumental backgrounds. The three dominant physics backgrounds are (i)  $Z \rightarrow \nu\bar{\nu} + \text{jets}$ , (ii)  $W \rightarrow \tau\nu + \text{jets}$ , where the  $\tau$  decays hadronically, and (iii)  $t\bar{t} \rightarrow \tau +$

jets, where the  $\tau$  decays hadronically. The  $\cancel{E}_T$  in leptonic  $W$  decays peaks at  $M_W/2 \simeq 40$  GeV, with a long tail at high  $\cancel{E}_T$  due to off-shell or high- $p_T$   $W$ 's and energy mismeasurements, so a large  $\cancel{E}_T$  cut is needed to remove these events. Instrumental backgrounds come from mismeasured vector boson,  $t$ , and QCD multijet events. Backgrounds from vector boson and  $t$  production occur for  $W \rightarrow e\nu, \mu\nu + \text{jets}$  events when the lepton is lost in a crack or is misidentified as a jet. QCD multijet production is a background when jet energy mismeasurements cause false  $\cancel{E}_T$ .

The DØ Run Ia analysis<sup>31</sup> searches for events with 3 or more jets and  $\cancel{E}_T$  and with 4 or more jets and  $\cancel{E}_T$ . Jets have  $E_T > 20$  GeV and cannot point along the  $\cancel{E}_T$  to avoid backgrounds from energy mismeasurement. The  $\cancel{E}_T$  threshold is 65 GeV and leptons are vetoed to remove  $W$  backgrounds. The resulting mass limits on  $\tilde{Q}$ 's and  $\tilde{g}$ 's are shown in Fig. 4 ((right), the plot containing the CDF results also shows the DØ Ia results); these limits were set using a RIPS model with the parameters  $M_{H^\pm} = 500$  GeV,  $\tan\beta = 2$ ,  $\mu = -250$  GeV, and  $M_{\tilde{\ell}} = m_{\tilde{Q}}$ .<sup>g</sup>

DØ also has a 3-jet analysis<sup>32</sup> based on 79.2 pb<sup>-1</sup> of Run Ib data. Jets must have  $E_T > 25$  GeV; the leading jet must have  $E_T > 115$  GeV because the only available unbiased sample to study the QCD multijet background had this requirement. The  $\cancel{E}_T$  cut ranges from 75 – 100 GeV and the  $H_T$  (scalar sum of the non-leading jet  $E_T$ 's) cut ranges from 100 – 160 GeV, optimized for each point in parameter space. Vector boson backgrounds are estimated using VECBOS<sup>33</sup> while the  $t\bar{t}$  background uses HERWIG<sup>34</sup> normalized to the DØ measured  $t\bar{t}$  cross section. Two techniques were used to calculate the QCD multijet background. One compares the opening angle between the two leading jets and the  $\cancel{E}_T$  in the signal sample to the analogous distribution in a generic multi-jet sample. The other selects events from a single jet trigger which pass all the selection criteria except for the  $\cancel{E}_T$  requirement. The  $\cancel{E}_T$  distribution is fit in the low  $\cancel{E}_T$  region, and extrapolated into the signal region. The background estimates can be found in Table 2.

The DØ data have been analyzed in the context of a mSUGRA model. For fixed  $\tan\beta$ ,  $A_0$ , and sign of  $\mu$ , exclusion curves are plotted in the  $m_0 - m_{1/2}$  plane (Fig. 4 (left)). The limits are from the 3-jet, 79.2pb<sup>-1</sup>, analysis only.<sup>h</sup> For each point in the limit plane, the  $\cancel{E}_T$  and  $H_T$  cuts are reoptimized based on the predicted background and SUSY signal. These results are robust within the mSUGRA framework.<sup>32</sup>

The CDF analysis of the Run Ib data set is not yet finished, but the Run Ia

---

<sup>g</sup>The efficiency and theoretical cross sections were calculated using ISAJET assuming 5 flavors of mass degenerate  $\tilde{Q}$ 's without  $\tilde{t}$  production.

result based on  $19 \text{ pb}^{-1}$  has been published.<sup>35</sup> The basic requirements are 3 or 4 jets with  $E_T > 15 \text{ GeV}$  and  $\cancel{E}_T > 60 \text{ GeV}$ . The vector boson backgrounds are estimated using **VECBOS** normalized to the CDF  $Wjj$  data. The  $t\bar{t}$  backgrounds are determined using **ISAJET** normalized to the CDF measured cross section. The QCD background is estimated using an independent data sample based on a trigger that required one jet with  $E_T > 50 \text{ GeV}$ . First all analysis cuts are applied to this sample except for the  $S$  cut, the  $\cancel{E}_T$  cut, and the 3 or 4 jets cut. Next the  $\cancel{E}_T$  distribution is fit and the number of events expected to pass the  $\cancel{E}_T$  cut is derived. Finally the efficiency of the last three cuts is applied to arrive at the final background estimate, shown in Table 2.

The limits derived from the CDF analysis are shown in Fig. 4 (right) within the RIPS framework. In RIPS, a heavy  $\tilde{g}$  implies a heavy  $\tilde{\chi}_1^0$ , so a light  $\tilde{Q}$  ( $m_{\tilde{Q}} \approx M_{\tilde{\chi}_1^0}$ ) decay will not produce much  $\cancel{E}_T$ . The consequence is an apparent hole in the CDF limit for small  $m_{\tilde{Q}}$  and large  $M_{\tilde{g}}$ . However, lighter  $\tilde{g}$ 's produce a large  $\cancel{E}_T$  because of the enforced mass splitting between the  $\tilde{g}$  and  $\tilde{\chi}_1^0$ . The results of this analysis do not change substantially as parameters are varied within the RIPS framework.<sup>35</sup>

Table 2: The number of expected and observed events for Tevatron  $\tilde{Q}$  and  $\tilde{g}$  searches in the jets+ $\cancel{E}_T$  channels.

|  | DØ                      |               | CDF                     |                       |
|--|-------------------------|---------------|-------------------------|-----------------------|
| Analysis                                     | 3 jets                  | 4 jets        | 3 or 4 jets             | 4 jets                |
| $\int \mathcal{L} dt (\text{pb}^{-1})$       | 79.2                    | 13.5          | 19                      | 19                    |
| $W^\pm$                                      | $1.56 \pm .67 \pm .42$  | $4.2 \pm 1.2$ | $13.9 \pm 2.1 \pm 6.0$  | $2.6 \pm 0.9 \pm 1.7$ |
| $Z \rightarrow \ell\bar{\ell}, \nu\bar{\nu}$ | $1.11 \pm .83 \pm .36$  | $1.0 \pm 0.4$ | $5.0 \pm 0.9 \pm 2.7$   | $0.4 \pm 0.2 \pm 0.4$ |
| $t\bar{t}$                                   | $3.11 \pm .17 \pm 1.35$ | –             | $4.2 \pm 0.3 \pm 0.5$   | $2.2 \pm 0.2 \pm 0.4$ |
| QCD multijets                                | $3.54 \pm 2.64$         | $1.6 \pm 0.9$ | $10.2 \pm 10.7 \pm 4.2$ | $3.2 \pm 3.8 \pm 1.3$ |
| Total Background                             | $9.3 \pm 0.8 \pm 3.3$   | $6.8 \pm 2.4$ | $33.5 \pm 11 \pm 16$    | $8 \pm 4 \pm 4$       |
| Events Observed                              | <b>15</b>               | <b>5</b>      | <b>24</b>               | <b>6</b>              |

**Dileptons+ $\cancel{E}_T$ :** If, in the cascade decay chain of the  $\tilde{Q}$ 's and  $\tilde{g}$ 's, there are two decays  $\tilde{\chi}_1^\pm \rightarrow \ell\nu\tilde{\chi}_1^0$ , or one decay  $\tilde{\chi}_2^0 \rightarrow \ell^+\ell^-\tilde{\chi}_1^0$ , the final state can contain 2 leptons, jets, and  $\cancel{E}_T$ , which is a relatively clean experimental signature. The requirement of two leptons significantly reduces jet backgrounds and removes most of the  $W$  backgrounds. Cutting on lepton pairs with the  $Z$  mass removes most of the  $Z$  backgrounds. If the leptons are required to have  $p_T > 20 \text{ GeV}$ , the major background from physics processes is  $t\bar{t} \rightarrow bW^+\bar{b}W^- \rightarrow b\bar{b}\ell^+\ell^- \cancel{E}_T$ . As the cut on lepton  $p_T$  is lowered,  $Z \rightarrow \tau^+\tau^-$ , where the  $\tau$ 's decay semileptonically, also becomes an important background. The instrumental backgrounds

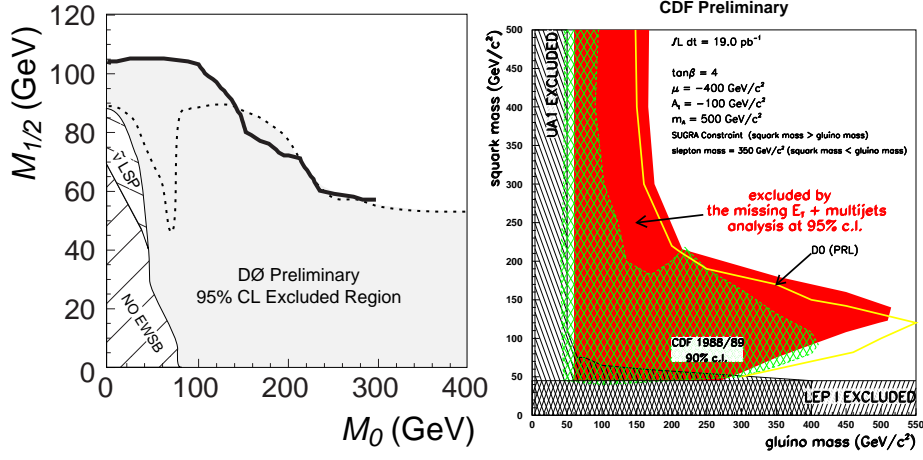


Figure 4: (Left) The DØ Excluded region in the  $m_0 - m_{1/2}$  plane with fixed parameters  $\tan\beta = 2$ ,  $A_0 = 0$ , and  $\mu < 0$ . The heavy solid line is the limit contour of the DØ jets and  $\cancel{E}_T$  analysis. The dashed line is the limit contour of the DØ dielectron analysis. The lower hashed area is a region where mSUGRA does not predict EWSB correctly. The hashed region above is where the  $\tilde{\nu}$  is the LSP. (Right) The CDF mass limits on  $\tilde{Q}$ 's and  $\tilde{g}$ 's from the search in jets and  $\cancel{E}_T$ <sup>35</sup> using  $19 \text{ pb}^{-1}$  of data and the ISAJET 7.06 Run I Parameter Set (RIPS) with the indicated values (solid area). For  $m_{\tilde{Q}} < M_{\tilde{g}}$ , the cross section used is LO, and 3 or more jets are required. For  $M_{\tilde{g}} < m_{\tilde{Q}}$ , the cross section is NLO,<sup>28</sup> and four jets are required. The line labelled “DØ PRL” is the DØ result from Run Ia using  $13.5 \text{ pb}^{-1}$  of data.<sup>31</sup>

are small. The spectacular signature of *like-sign*, isolated dileptons, which is difficult to produce in the SM, can occur whenever a  $\tilde{g}$  is produced directly or in a cascade decay, since the  $\tilde{g}$  is a Majorana particle. This property is exploited in the CDF dilepton searches.

The DØ analysis ( $e$  only) requires two leptons,  $E_T > 15 \text{ GeV}$ , of any sign, while the CDF analysis ( $e$  and  $\mu$ ) requires two leptons  $E_T > 11.5 \text{ GeV}$ , with the same sign. Both analyses require  $\cancel{E}_T > 25 \text{ GeV}$ . Figure 5 shows the the DØ<sup>36</sup> results from Run Ib, plotted for mSUGRA models in the  $m_0 - m_{1/2}$  plane. Figure 6 ((left), dark shading) shows the CDF<sup>38,37</sup> result plotted in the  $M_{\tilde{g}} - m_{\tilde{Q}}$  plane for a RIPS model, and (right) a mapping of the DØ mSUGRA results from Fig. 5 (left) into the same coordinates. The CDF limit is based on NLO cross sections,<sup>28</sup> and the DØ limit on LO cross sections. The DØ limits on  $m_0$  and  $m_{1/2}$  are calculated including contributions from the production of all sparticles (for instance, associated production of  $\tilde{\chi}^0$ 's or  $\tilde{\chi}^\pm$ 's with  $\tilde{Q}$ 's or  $\tilde{g}$ 's),

while the CDF result considers only  $\tilde{Q}$  and  $\tilde{g}$  production.

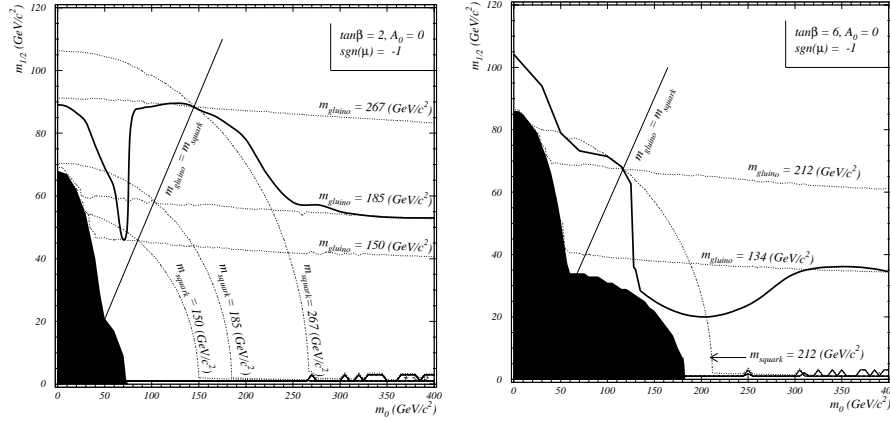


Figure 5: (Left) The DØ limits on the SUGRA parameters  $m_0$  and  $m_{1/2}$  from the 2 leptons, 2 jets, and  $\cancel{E}_T$  search<sup>36</sup> for  $\tan\beta=2$ ,  $A_0=0$ , and  $\mu < 0$ . (Right) The same plot for  $\tan\beta=6$ ,  $A_0=0$ , and  $\mu < 0$ . In both plots, the dark shaded area is the region in which electroweak symmetry breaking is not realized. Selected contours of  $\tilde{Q}$  and  $\tilde{g}$  mass are also shown.

For  $m_{\tilde{Q}} \gg M_{\tilde{g}}$  or, equivalently, for  $m_0 \gg m_{1/2}$ ,  $\tilde{g}\tilde{g}$  pair production is the dominant SUSY process. As  $m_0(m_{\tilde{Q}})$  is varied with the other parameters fixed, the branching ratios for the 3-body  $\tilde{g}$  decays to  $\tilde{\chi}^\pm$ 's or  $\tilde{\chi}^0$ 's and jets become fairly constant, so the production rate of leptonic final states becomes constant. For large enough values of the  $\tilde{g}$  mass, the leptons easily pass the experimental cuts, and the experimental limit approaches a constant value asymptotically, as can be seen in both the DØ and CDF plots shown in Fig. 6.

The relation  $m_{\tilde{Q}} \ll M_{\tilde{g}}$  is not possible in SUGRA, and is treated in an *ad hoc* manner in RIPS. There is no limit in this region for either opposite- or like-sign dilepton pairs because the large, fixed  $\tilde{\ell}$  masses (as assumed in this analysis) limit the branching ratios to leptonic final states. The possibility of like-sign dilepton pairs is further reduced because both the  $\tilde{g}\tilde{g}$  and  $\tilde{g}\tilde{Q}$  cross sections (which produce like-sign leptons because the  $\tilde{g}$  is a Majorana particle) and the  $\tilde{Q}\tilde{Q}$  cross section (which produces like-sign leptons because the  $\tilde{Q}$ 's have the same charge) are small in this region.

When  $m_{\tilde{Q}} \simeq M_{\tilde{g}}$ , the  $\tilde{g}\tilde{g}$  cross section is supplemented by the  $\tilde{g}\tilde{Q}$  cross section. Just above the diagonal line at  $M_{\tilde{g}} = m_{\tilde{Q}}$  (*i.e.*  $m_{\tilde{Q}}$  just larger than  $M_{\tilde{g}}$ ) in Fig. 6 there are “noses” in the limit plots, with the limit becoming

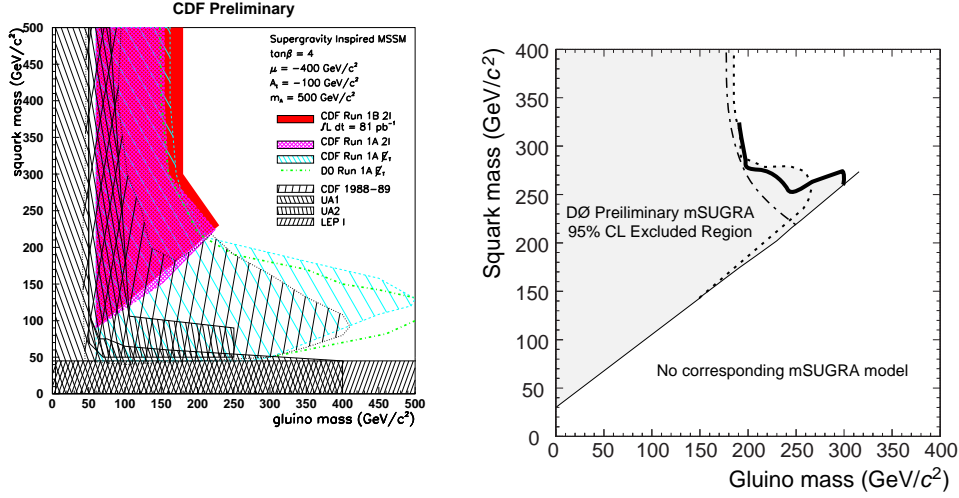


Figure 6: (Left) CDF limits on the  $\tilde{Q}$  and  $\tilde{g}$  masses from the 2 like-sign leptons, 2 jets, and  $\cancel{E}_T$  search in  $81 \text{ pb}^{-1}$  (dark shading). The limits were set using the ISAJET 7.06 Run I Parameter Set (RIPS) with the indicated values. (Right) Excluded region from various DØ analyses in the  $m_{\tilde{Q}} - M_{\tilde{g}}$  plane with fixed mSUGRA parameters  $\tan \beta = 2$ ,  $A_0 = 0$ , and  $\mu < 0$ . There are no mSUGRA models in the region to the right of the diagonal thin line. The heavy solid line is the limit contour of the DØ Run Ib 3 jets and  $\cancel{E}_T$  analysis. The dashed line is the limit contour of the DØ Run Ib dielectron analysis. The dot-dashed line is the limit contour of the DØ Run Ia 3 and 4 jets and missing transverse energy analysis shown only in the region with valid mSUGRA models.

stronger close to the diagonal.

The limits in Fig. 6 are for a specific choice of parameters within RIPS or mSUGRA. If  $\mu$ ,  $A_t$  and  $\tan \beta$  are varied, the branching ratios into  $\tilde{\chi}^\pm$ 's or  $\tilde{\chi}^0$ 's can vary strongly. The sensitive dependence on the parameters can be seen within mSUGRA from the DØ limits in Fig. 5. The dip in the  $\tan \beta = 2$  limit (left), around  $m_0 = 70 \text{ GeV}$ , is a point where  $m_{\tilde{t}} > M_{\tilde{\chi}_2^0} > m_{\tilde{\nu}}$  and  $\text{BR}(\tilde{\chi}_2^0 \rightarrow \nu \tilde{\chi}_1^0) \simeq 1$ , so the detection efficiency is very sensitive to the choice of high energy parameters  $m_0$  and  $m_{1/2}$ . In Fig. 5 (right), with  $\tan \beta = 6$ , the limits are severely reduced compared to Fig. 5 (left), with  $\tan \beta = 2$ , in the region where  $m_{\tilde{Q}} \gg M_{\tilde{g}}$ . For large  $\tan \beta$ , the mass splittings are reduced, and the leptons from the  $\tilde{\chi}_1^\pm$  and  $\tilde{\chi}_2^0$  decays are softer. The non-trivial shape of the limit curves results from an interplay between the cross section being larger when

$m_0$  and  $m_{1/2}$  are smaller (sparticle masses are smaller) and the mass splittings being smaller. Consequently, although the dileptons+jets+ $\cancel{E}_T$  signature is an excellent discovery channel with little SM background, it is hard to set significant parameter limits even using mSUGRA models.

From the present analyses in the  $\cancel{E}_T$ +jets and dileptons+ $\cancel{E}_T$  channels, some preliminary conclusions can be drawn on the  $\tilde{Q}$  and  $\tilde{g}$  masses. These depend, however, on the assumed SUSY parameters. The  $D\bar{O}$  limit on the  $\tilde{g}$  mass effectively develops a plateau at 185 GeV for large  $m_0$  and  $\tan\beta=2$ , and at 134 GeV for  $\tan\beta=6$ . The CDF limit on the  $\tilde{g}$  mass is 180 GeV for  $\tan\beta=4$  and large  $m_{\tilde{Q}}$ . For equal  $\tilde{Q}$  and  $\tilde{g}$  masses, the  $D\bar{O}$  mass limit for  $\tan\beta=2$  is 267 GeV. From the CDF RIPS analyses and  $m_{\tilde{Q}} \simeq M_{\tilde{g}}$ , the limit is about 220 GeV for  $\tan\beta=4$ . A direct comparison of all the above results is rather difficult since  $D\bar{O}$  and CDF have done analyses assuming different sets of MSSM parameters.

**Stop Squarks:** The top squark (stop) is a special case.<sup>39,40</sup> The mass degeneracy in the  $\tilde{t}$  sector is expected to be strongly broken, and, for sufficiently large mixing, the lightest stop  $\tilde{t}_1$  can be rather light, possibly lighter than the  $\tilde{\chi}_1^\pm$ . The  $\tilde{t}_1$  has about a tenth the production cross section<sup>28</sup> of a  $t$  quark of the same mass, because the cross section behaves as  $\beta^3$  at threshold (compared to  $\beta$  for fermion pairs), where  $\beta$  is the squark velocity in the rest frame of the pair, and only half the scalar partners are being considered.

The stop can be produced directly as  $\tilde{t}\tilde{t}^*$  pairs or, depending on the  $\tilde{t}$  mass, indirectly in decays  $t \rightarrow \tilde{t}\tilde{\chi}_1^0$ , or  $\tilde{\chi}_i^\pm \rightarrow b\tilde{t}$ . Also depending on the  $\tilde{t}$  mass, one of three decay modes is expected to dominate. If (a)  $m_{\tilde{t}_1} > m_{\tilde{\chi}_1^\pm} + m_b$ , then  $\tilde{t}_1$  can decay into  $b\tilde{\chi}_1^\pm$ , followed by the decay of the  $\tilde{\chi}_1^\pm$ . This can look similar to the decay  $t \rightarrow bW$ , but with different kinematics and branching ratios for the final state. Instead, if  $\tilde{t}_1$  is the lightest charged SUSY particle, it is expected to decay exclusively through a  $\tilde{\chi}^\pm - \tilde{b}$  loop as (b)  $\tilde{t}_1 \rightarrow c\tilde{\chi}_1^0$ , which looks quite different from SM top decays. Finally, the  $\tilde{t}$  can decay (c)  $\tilde{t} \rightarrow bW\tilde{\chi}_1^0$  or, if it is quite heavy,  $\tilde{t} \rightarrow t\tilde{\chi}_1^0$ .

$D\bar{O}$  has searched for  $\tilde{t}\tilde{t}^*$  production with  $\tilde{t} \rightarrow c\tilde{\chi}_1^0$  using 7.4 pb<sup>-1</sup> of Run Ia data.<sup>41</sup> The signature used is two acollinear jets,  $E_T > 30$  GeV and  $\cancel{E}_T > 40$  GeV. The dijet cross section is large, and thus this signature has large instrumental backgrounds. It also has backgrounds from vector boson production. The multijet backgrounds can be controlled by requiring  $\Delta\phi > 45^\circ$  between the  $\cancel{E}_T$  and each jet, and that the jets not be back-to-back. The vector boson backgrounds are controlled by requiring that the two leading jets are separated by at least  $\Delta\phi > 90^\circ$ . After these cuts, the dominant backgrounds are from  $W$  and  $Z$  boson production and decay, with the largest being  $W \rightarrow \tau\nu$ .



The efficiency is largest when the stop is heavy compared to the  $\tilde{\chi}_1^0$  (near the kinematic boundary for the decay  $\tilde{t}_1 \rightarrow bW^+\tilde{\chi}_1^0$ ), reaching a maximum value of only 4%. The mass difference  $m_{\tilde{t}} - M_{\tilde{\chi}_1^0}$  determines the  $E_T$  of the charm jet and rapidly limits this search mode as the  $c$ -jets become too soft (see Fig. 7). With the assumption that  $\text{BR}(\tilde{t}_1 \rightarrow c\tilde{\chi}_1^0)=1$ , the predicted SUSY final state depends only on  $M_{\tilde{\chi}_1^0}$  and  $m_{\tilde{t}_1}$ . The result of this search is a 95% C.L. exclusion limit on a region in the  $M_{\tilde{\chi}_1^0} - m_{\tilde{t}_1}$  plane, shown in Fig. 7.<sup>h</sup>

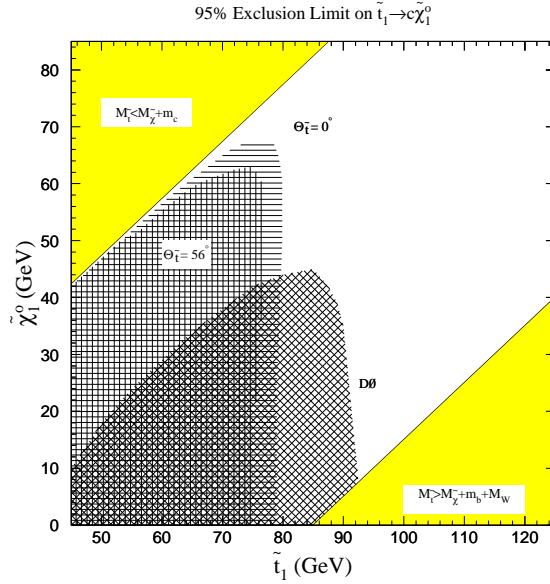


Figure 7: Mass limits from the  $D\bar{O}$  search for  $\tilde{t}\tilde{t}^*$  production with the decay  $\tilde{t} \rightarrow c\tilde{\chi}_1^0$  at the Tevatron.<sup>41</sup> The decay is kinematically forbidden in the two solid grey regions. The hashed regions marked  $\Theta_{\tilde{t}}$  show the LEP excluded regions as a function of the  $\tilde{t}$  mixing angle, which determines the strength of the  $\tilde{t}$  coupling to the  $Z$ . The mixing does not affect the tree level process at hadron colliders.

CDF and  $D\bar{O}$  have also presented results from a search for  $\tilde{t}_1\tilde{t}_1^*$  production, with  $\tilde{t}_1 \rightarrow b\tilde{\chi}_1^\pm$ . The CDF search is in the lepton+jets channel, and uses a shape analysis of the transverse mass of the lepton ( $E_T > 20$  GeV) and  $\cancel{E}_T (> 20$  GeV).<sup>42</sup> The results of the CDF search are shown in Fig. 8 (left).

<sup>h</sup>The production rate has been calculated using only LO production cross sections from ISAJET.

The decay  $\tilde{\chi}_1^\pm \rightarrow W^* \tilde{\chi}_1^0$  is assumed using the masses (i)  $M_{\tilde{\chi}_1^\pm} = 80$  GeV and  $M_{\tilde{\chi}_1^0} = 30$  GeV and (ii)  $M_{\tilde{\chi}_1^\pm} = 70$  GeV and  $M_{\tilde{\chi}_1^0} = 30$  GeV.<sup>i</sup> Given these mass choices, there is little other parameter dependence. Presently, the cross section limits are above the predicted cross sections due to the high  $E_T$  cuts.

DØ searches in the dilepton channel<sup>43</sup> ( $E_T > 16.8$  GeV) and  $\cancel{E}_T > 22$  GeV. The results are shown in Fig. 8 (right), assuming  $M_{\tilde{\chi}_1^\pm} = 47$  GeV and  $M_{\tilde{\chi}_1^0} = 28.5$  GeV. A substantial background comes from  $Z \rightarrow \tau^+ \tau^-$ , again requiring a high threshold for the  $E_T$  cuts, and no limit can be set.<sup>j</sup>

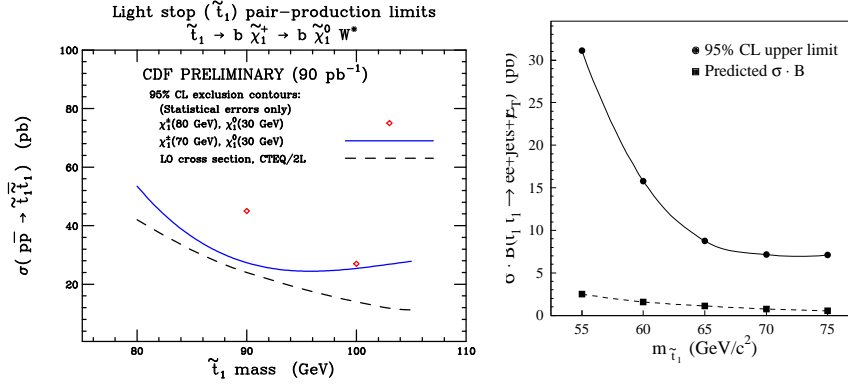


Figure 8: (Left) The CDF cross section limit on direct production of the top squark using 90  $\text{pb}^{-1}$  of data. The decay mode is  $\tilde{t} \rightarrow b\tilde{\chi}_1^+ (\rightarrow W^* \tilde{\chi}_1^0)$ . One  $W$  must decay semi-leptonically giving a signature of a lepton,  $\cancel{E}_T$ , and jets. The theoretical cross section is from ISAJET 7.06. (Right) The DØ 95% confidence level cross section limit on the cross section for stop production times the branching ratio to a final state containing 2 electrons as a function of the mass of the  $\tilde{t}$  is shown as a solid line.<sup>43</sup> The mass of the lightest chargino is assumed to be 47 GeV. The predicted cross section times branching ratio from ISAJET is also shown as a dashed line.

CDF has presented another analysis using the SVX-tagged lepton+jets sample to search for the decay  $t \rightarrow \tilde{t}_1 \tilde{\chi}_1^0$ , with  $\tilde{t}_1 \rightarrow b\tilde{\chi}_1^\pm$ .<sup>44</sup> If one  $t$  in a  $t\bar{t}$  event decays  $t \rightarrow bW (\rightarrow \ell\nu)$  and the other  $t \rightarrow \tilde{t}_1 \tilde{\chi}_1^0$  followed by  $\tilde{t}_1 \rightarrow b\tilde{\chi}_1^\pm (\rightarrow jj\tilde{\chi}_1^0)$  or  $t \rightarrow bW (\rightarrow jj)$  and  $t \rightarrow \tilde{t}_1 \tilde{\chi}_1^0$  followed by  $\tilde{t}_1 \rightarrow b\tilde{\chi}_1^\pm (\rightarrow \ell\nu\tilde{\chi}_1^0)$ , the signature is  $b\bar{b}\ell\nu jj + \cancel{E}_T$ , the same as in the SM, but where the  $\cancel{E}_T$  includes the momentum of the  $\tilde{\chi}_1^0$ . The cuts, lepton  $E_T > 20$  GeV,  $\cancel{E}_T > 45$  GeV, and one SVX  $b$ -tag, are optimized for acceptance of the SUSY decay and rejection

<sup>i</sup>This analysis was done in regions of MSSM parameter space later excluded by LEP. It demonstrates, however, the procedures to be followed in performing these studies in other regions.

of  $W$ +jets background. A likelihood function is computed for each event reflecting the probability that the jets with the 2<sup>nd</sup> and 3<sup>rd</sup> highest  $E_T$  in the event are consistent with the stiffer SM distribution (as compared to the SUSY distribution). The distribution of this likelihood function shows a significant separation of these two hypotheses. After applying the cuts, 9 events remain, all of which fall outside of the SUSY signal region. For  $\hat{t}$  masses between 80 and 150 GeV and  $\tilde{\chi}^\pm$  masses between 50 and 135 GeV, a  $\text{BR}(t \rightarrow \tilde{t}_1 \tilde{\chi}_1^0) = 50\%$  is excluded at the 95% C.L., provided that  $M_{\tilde{\chi}_1^0} = 20$  GeV.<sup>j</sup> Because  $M_{\tilde{\chi}_1^0}$  is fixed in this manner, it is not related to  $M_{\tilde{\chi}_1^\pm}$  as in SUGRA.

### 3.3 Sleptons

At hadron colliders,  $\tilde{\ell}$ 's and  $\tilde{\nu}$ 's can only be directly produced through their electroweak couplings to the  $\gamma$ ,  $Z$  and  $W$  bosons. The production cross sections are at most a few tens or hundreds of fb at the Tevatron,<sup>45</sup> and the physics and instrumental backgrounds are numerous. So far neither collaboration has presented results on searches for sleptons in the SUGRA or RIPS framework (we describe limits in gauge-mediated SUSY models later).

A (stable) charged slepton is not a viable LSP candidate, so the decays  $\tilde{\ell}_{L,R}^\pm \rightarrow \ell^\pm \tilde{\chi}_i^0$  or  $\tilde{\ell}_L^\pm \rightarrow \nu \tilde{\chi}_i^\pm$  are expected. A  $\tilde{\nu}$ , instead, can be the LSP, or it can decay invisibly  $\tilde{\nu} \rightarrow \nu \tilde{\chi}_1^0$ , or visibly  $\tilde{\nu} \rightarrow \tilde{\chi}_i^\pm \ell^\mp$ . If  $m_{\tilde{\nu}} < m_{\tilde{\ell}} < M_{\tilde{\chi}_1^0}$ , then the decay  $\tilde{\ell} \rightarrow \ell' \nu' \tilde{\nu}$  (or  $\tilde{\ell} \rightarrow q \bar{q} \tilde{\nu}$ ) is possible. Promising signatures are (i)  $e^+e^-$ ,  $\mu^+\mu^-$ ,  $\tau^+\tau^- + \cancel{E}_T$ , (ii)  $e\mu$ ,  $e\tau$ ,  $\mu\tau + \cancel{E}_T$ , and (iii)  $e$ ,  $\mu$  or  $\tau$ +jets +  $\cancel{E}_T$  (or jets +  $\cancel{E}_T$ ). Although charged slepton production can lead to charged leptons in the final state, there is no guarantee.

### 3.4 Charged Higgs Bosons

Even though Higgs bosons are not sparticles, the discovery of one or more could be considered *indirect* evidence for SUSY. If it is light enough, the  $H^\pm$  can be produced in the decay  $t \rightarrow bH^+$ .<sup>46</sup> The branching fraction for this decay depends on the  $H^\pm$  mass and  $\tan\beta$ , and is larger than 50% for  $\tan\beta$  less than approximately 0.7 or greater than approximately 50, but very small or large values of  $\tan\beta$  are theoretically disfavored. In general, at reasonably small values of  $\tan\beta$ ,  $H^+ \rightarrow c\bar{s}$ ; at large  $\tan\beta$ ,  $H^+ \rightarrow \tau^+\nu_\tau$ .

CDF has searched for the decay  $t \rightarrow bH^+$  using both direct<sup>47,48</sup> and indirect<sup>23</sup> methods. Direct searches look for an excess over SM expectations of events with  $\tau$  leptons from the decay  $H^+ \rightarrow \tau^+\nu_\tau$  (dominant for large  $\tan\beta$ ). The signature for hadronically decaying  $\tau$ 's is a narrow jet associated with

one or three tracks with no other tracks nearby. Indirect searches are “disappearance” experiments, relying on the fact that decays  $t \rightarrow bH^+$  will deplete the SM decays  $t \rightarrow bW$ , decreasing the number of events in the dilepton and lepton+jets channels.

The selection criteria for the CDF direct search are either a single  $\tau$ ,  $E_T > 20$  GeV,  $\cancel{E}_T > 30$  GeV and a SVX  $b$ -tagged jet, or two  $\tau$ 's, with  $E_T > 30$  GeV. Values of  $m_{H^\pm}$  and  $\tan\beta$  can be excluded based on two methods: either the model is inconsistent with the observation of  $\tau$ 's, (Fig. 9 (left)), or the model is inconsistent with the combination of the number of  $\tau$  events and the number of lepton+jets events. The second method has the advantage that a  $t\bar{t}$  cross section  $\sigma_{t\bar{t}}$  does not need to be assumed; details are presented elsewhere.<sup>48</sup> The reader should be aware that there are subtleties in analyses that assume cross sections.<sup>3</sup>

A direct search at small  $\tan\beta$  is difficult since the  $H^\pm$  would decay into two jets. However, the indirect method can be applied to both small and large  $\tan\beta$  searches. If a choice of  $\sigma_{t\bar{t}}$ ,  $m_{H^\pm}$ , and  $\tan\beta$  predicts a number of dilepton and lepton+jets events that is inconsistent with the observations, then that set of values is excluded (Fig. 9 (left)). The area in Fig. 9 (left) labeled “ratio method” is the exclusion region for an indirect search that does not make an assumption for  $\sigma_{t\bar{t}}$ . The limit is set by comparing the ratio of dilepton to lepton+jets events, since  $t \rightarrow bH^+$  decays always decreases this ratio, regardless of  $\sigma_{t\bar{t}}$ .

Recent studies have shown that quantum SUSY effects (SUSY QCD and electroweak radiative corrections) to the decay mode  $t \rightarrow bH^+$  (with subsequent decays into  $\tau$ 's) may be important and should be considered in future analyses.<sup>50</sup>

### 3.5 Neutral Higgs Bosons

The lightest CP-even Higgs boson  $h$  can be produced at the Tevatron in the channels  $Wh$  or  $Zh$ .<sup>7</sup> These channels are relevant for large values of  $M_A$  (the SM limit) or for small  $M_A$  and small  $\tan\beta$ . The heavier Higgs  $H$  could become relevant for searches at an upgraded Tevatron through  $ZH$ ,  $WH$  production, in some restricted region of parameter space, complementary to the one relevant for the  $h$  searches. In addition, the enhancement of the  $b$  Yukawa coupling for large  $\tan\beta$  can enhance  $hb\bar{b}$ ,  $Ab\bar{b}$ , and  $Hb\bar{b}$  production.<sup>51</sup>

Both collaborations have searched for  $q\bar{q}' \rightarrow W^* \rightarrow W(\rightarrow e\nu, \mu\nu)h(\rightarrow b\bar{b})$ . DØ has searched in 100 pb<sup>-1</sup> of data using a data sample containing a lepton ( $E_T > 20$  GeV),  $\cancel{E}_T (> 20$  GeV) and two jets.<sup>52</sup> One of the jets must have a muon associated with it for  $b$ -tagging. Twenty-seven events pass the selection

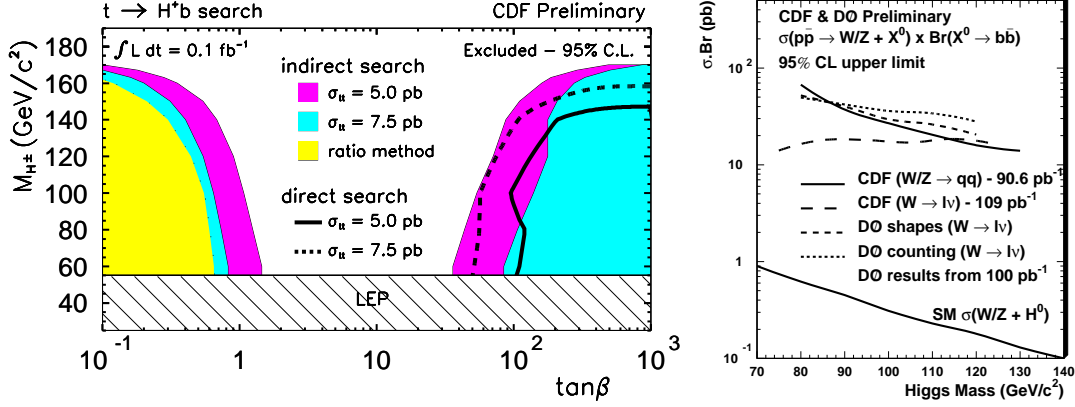


Figure 9: (Left) Exclusion space for the CDF searches for decays  $t \rightarrow bH^+$  in  $t\bar{t}$  events. The region excluded with solid lines at high  $\tan\beta$  is from a direct search for events where one or both  $t$ 's in a  $t\bar{t}$  event decay to  $bH^+(\rightarrow \tau^+\nu)$  and information from the SM channels is ignored. The shaded regions are from the indirect searches. For the regions labeled  $\sigma_{t\bar{t}} = 5.0$  and 7.5 pb,  $\sigma_{t\bar{t}}$  is assumed and points are excluded if the predicted SUSY decays have depleted the SM channels to an extent that they are inconsistent with the data. The “ratio method” is an indirect method comparing the ratio of lepton+jets to dilepton events and no  $\sigma_{t\bar{t}}$  is assumed. (Right) Limits from CDF and D0 for the associated production of  $Wh$  or  $Zh$ . The CDF limits are shown for the final states of  $\ell\nu b\bar{b}$  and  $j\bar{j}b\bar{b}$ , and the D0 limit is for the final state  $\ell\nu b\bar{b}$ . The limit is set using a simple counting method and by fitting the  $b\bar{b}$  spectrum (“shapes”).

criteria;  $25.5 \pm 3$  events are expected from  $Wj\bar{j}$  and  $t\bar{t}$ . The limits shown in Fig. 9 (right) are set by a simple event-counting method and by fitting the  $b\bar{b}$  dijet mass spectrum.

CDF has recently completed a similar search for the same decay mode using 109 pb<sup>-1</sup> of data.<sup>53</sup> Leptons must have  $E_T > 25$  (e) or 20 GeV ( $\mu$ ) and the event must have  $\cancel{E}_T > 25$  (e) or 20 GeV ( $\mu$ ) and one SVX  $b$ -tag. These events are split into single-tagged (one SVX tag) and double-tagged samples (two SVX tags or one SVX and one lepton ( $e$  or  $\mu$ ) tag). The 36 (6) single-tagged (double-tagged) events are consistent with the  $30 \pm 5$  ( $3.0 \pm 0.6$ ) expected from SM  $W$ +jets and  $t\bar{t}$ . Both the single- and double-tagged dijet mass distributions are fit simultaneously to set the limits shown in Fig. 9 (right).

The process  $q\bar{q} \rightarrow Z^* \rightarrow Zh$  occurs at a comparable rate to the  $W^*$  process. CDF has searched for both processes assuming  $W/Z \rightarrow j\bar{j}$ .<sup>54</sup> All events must have 4 jets with  $E_T > 15$  GeV and two SVX  $b$ -tags. In 91 pb<sup>-1</sup> of data,

589 events remain, consistent with the expectation from QCD heavy-flavor production and fake tags. To set limits, the  $b\bar{b}$  dijet mass spectrum is fit. Also shown in Fig. 9 (right) is the SM production cross section for  $Wh$  and  $Zh$  as a function of the Higgs boson mass. The present experimental limits are roughly two orders-of-magnitude away from the predicted cross section.

DØ has also searched for an  $h$  with suppressed couplings to fermions,<sup>55</sup> so that  $h \rightarrow \gamma\gamma$  can be dominant (see the first reference of [7]). Events are selected containing two photons with  $E_T > 20$  and 15 GeV, and two jets with  $E_T > 20$  and 15 GeV. No evidence of a resonance is seen in the mass distribution of the 2 photons, and DØ excludes such a Higgs with a mass less than 81 GeV at a 95% C.L.

### 3.6 R-Parity Violation

Allowing for  $\tilde{R}$  in the MSSM opens a host of possibilities at the Tevatron.<sup>60</sup> The possible excess of HERA events at large  $Q^2$  has triggered interest in studying the consequences of the interaction of a light  $\tilde{Q}$  (preferably a  $\tilde{t}$  or  $\tilde{c}$ ) with an electron and a  $d$  quark.<sup>62</sup> If the  $\tilde{g}$  were heavier than this  $\tilde{Q}$ , then  $\tilde{g}$  pair production at the Tevatron and the decay  $\tilde{g} \rightarrow \tilde{c}\tilde{c}_L$  through R-conserving couplings, followed by the  $\tilde{R}$  decay  $\tilde{c}_L \rightarrow e^+d$ , would yield the signature of two electrons and 4 jets.<sup>j</sup>

CDF has performed a search<sup>61</sup> considering the  $\tilde{R}\tilde{Q}$  decays with the signature of two like-sign electrons ( $E_T > 15$  GeV) and two jets ( $E_T > 15$  GeV). In 105 pb<sup>-1</sup> of Run Ia and Ib data, no events remain after all cuts are applied. Varying the masses of the SUSY particles does not alter the acceptance significantly since they are heavy enough for the decay products to easily pass the  $E_T$  thresholds. Because of this, the limit on the cross section times branching ratio is approximately constant at 0.19 pb. For  $m_{\tilde{c}_L} = 200$  GeV, this excludes  $M_{\tilde{g}} < 230$  GeV, assuming  $\text{BR}(\tilde{g}\tilde{g} \rightarrow e^\pm e^\pm X) = 1/8$ .

Allowing for R-parity conserving  $\tilde{Q}$  decays, the decay  $\tilde{Q} \rightarrow q\tilde{\chi}_1^0$  is possible, where  $\tilde{\chi}_1^0$  is the LSP. Since the LSP has no R-parity conserving decays kinematically accessible, the  $\tilde{R}$  decay  $\tilde{\chi}_1^0 \rightarrow c\tilde{d}e^-$  or  $\tilde{c}\tilde{d}e^+$  occurs through a virtual  $\tilde{c}$  or  $\tilde{d}$ , while  $\tilde{\chi}_1^0 \rightarrow d\tilde{s}\nu$  or  $\tilde{d}\tilde{s}\bar{\nu}$  occurs through a virtual  $\tilde{s}$  or  $\tilde{d}$ . For the analysis, 5  $\tilde{Q}$  masses are assumed to be degenerate, and  $\tilde{Q}$  masses less than 210 GeV are excluded if the mass of the  $\tilde{\chi}_1^0$  is more than half of the  $\tilde{Q}$  mass and the  $\tilde{g}$  is heavy.

If R-parity is violated, and the LSP is charged (*e.g.* a  $\tilde{\tau}$ ), it can be long-lived and appear as a heavy stable particle. The particle can be identified by

---

<sup>j</sup>If the above  $\tilde{R}$  decay is allowed, then the same  $\tilde{R}$  coupling will induce the decays  $\tilde{s}_L \rightarrow \nu_e d$ ,  $\tilde{d}_R \rightarrow e^- c$  and  $\tilde{d}_R \rightarrow \nu_e s$ .

measuring the  $dE/dx$  energy loss as it passes through the CDF SVX and CTC detectors. For a given momentum, a heavy particle has a slower velocity and hence a greater energy loss than a relativistic particle ( $\beta \simeq 1$ ). If the particle is weakly interacting or massive enough to kinematically suppress showering, it will penetrate the detectors and be triggered on and reconstructed as a muon with too much energy loss. A result using part of the Run I data has been presented by CDF<sup>59</sup> and is now updated with the full data set. In  $90 \text{ pb}^{-1}$  of inclusive muon triggers ( $p_T > 30 \text{ GeV}$ ), CDF searches for particles with ionization consistent with  $\beta\gamma < 0.6$  and finds 12 events depositing more than twice the energy expected from a minimum ionizing muon. This is consistent with the number of events expected from muons which overlap with other tracks to fake a large  $dE/dx$  signal.

### 3.7 Photon and $\cancel{E}_T$ Signatures

SUSY has so many parameters that the full range of its allowed signatures may be hard to predict. In April 1995, the CDF experiment recorded an event with a very unusual topology<sup>63</sup> which may have SUSY interpretations. It has four electromagnetic clusters, which pass the typical cuts for two electrons and two photons, and  $\cancel{E}_T$ .

There have been two main proposals for a possible SUSY explanation of the event: the Gravitino LSP and the Higgsino LSP model (there are also non-SUSY explanations<sup>64</sup>). In gauge-mediated SUSY models, the  $\tilde{G}$  is the LSP and the next-to-lightest superpartner (NLSP) decays into its SM partner plus the Goldstino component of the  $\tilde{G}$ .<sup>69</sup> If  $\tilde{\chi}_1^0$  is the NLSP, the only modification to SUGRA phenomenology, where all sparticles decay down to  $\tilde{\chi}_1^0$ , is that  $\tilde{\chi}_1^0$  then decays to a photon and  $\cancel{E}_T$ . In particular, the CDF event can be interpreted as either  $\tilde{e}\tilde{e}^*$  production<sup>65,68</sup> or  $\tilde{\chi}_1^+\tilde{\chi}_1^-$  production.<sup>68</sup>

The Higgsino LSP model<sup>66</sup> involves a region of MSSM parameter space in which the  $\tilde{\chi}_2^0$  is photino-like and the  $\tilde{\chi}_1^0$  is Higgsino-like, so the radiative decay  $\tilde{\chi}_2^0 \rightarrow \gamma\tilde{\chi}_1^0$  dominates over other  $\tilde{\chi}_2^0$  decay modes.<sup>72</sup> The event can be again interpreted as  $\tilde{e}\tilde{e}^*$  production or  $\tilde{\chi}_1^+\tilde{\chi}_1^-$  production.

Both proposals also suggest other signatures that should be expected within these models.<sup>67</sup> The  $\tilde{G}$  LSP model predicts a large number of events with many jets, leptons, and  $\gamma$ 's, and the fact that none of these other signatures has been detected makes the above LSP  $\tilde{G}$  explanation of the CDF  $ee\gamma\gamma\cancel{E}_T$  event unlikely.<sup>70,71</sup> In Higgsino LSP models,  $\gamma$ 's only arise from the decay of  $\tilde{\chi}_2^0$ , and there is no guarantee that there will be other substantial signals. A logical starting place for searches is in the inclusive two photon and  $\cancel{E}_T$  channel.<sup>70</sup> The generic  $\gamma\gamma\cancel{E}_T + X$  signature has no significant background

from real  $\gamma$ 's. The main backgrounds are caused by jets and electrons faking  $\gamma$ 's. The SM production of  $W(\rightarrow e\nu)\gamma + \text{jets}$  can fake some of the signatures if the electron is misidentified as a  $\gamma$ . These events have a  $\cancel{E}_T$  spectrum typical of  $W$  events, peaked at about  $M_W/2 \simeq 40$  GeV, with a long tail to high  $\cancel{E}_T$ . The dominant instrumental background, however, is from di-jet and  $\gamma$ +jet production, where the large production cross section overcomes the small probability ( $\simeq 10^{-4} - 10^{-3}$ ) that a jet fakes a  $\gamma$ .

Figure 10 shows the  $\cancel{E}_T$  distributions from DØ (left) and CDF (right) diphoton events<sup>74,75</sup> after imposing the selection criteria. The DØ analysis requires two  $\gamma$ 's with  $E_T > 20, 12$  GeV and  $\cancel{E}_T > 25$  GeV, while CDF requires two  $\gamma$ 's with  $E_T > 25$  GeV and  $\cancel{E}_T > 35$  GeV. For the DØ analysis, the shape of the  $\cancel{E}_T$  spectra agrees well with backgrounds containing two electromagnetic-like clusters, where at least one of the two clusters fails the  $\gamma$  selection criteria. Two events satisfy all selection criteria, with a predicted background, dominated by jets faking  $\gamma$ 's, of  $2.3 \pm 0.9$  events. For the CDF analysis, the shape of the  $\cancel{E}_T$  distribution is in good agreement with the resolution of the  $Z \rightarrow e^+e^-$  control sample. The event on the tail in  $\cancel{E}_T$  is the “ $ee\gamma\gamma\cancel{E}_T$ ” event. If the source of this event is an anomalously large  $WW\gamma\gamma$  production cross section that yields one event in  $\ell\ell\gamma\gamma\cancel{E}_T$ , CDF would expect dozens of events with two  $\gamma$ 's and several observed jets. However, the jet multiplicity spectrum in diphoton events is well-modeled by an exponential, and there are no diphoton events with 3 or 4 jets.

DØ presents limits<sup>75</sup> in the framework of the  $\tilde{G}$  LSP scenario by considering  $\tilde{\chi}^0$  and  $\tilde{\chi}^\pm$  pair production. Assuming  $M_2 \simeq 2M_1$  and large values of  $m_{\tilde{Q}}$ , the signatures are a function of only  $M_2$ ,  $\mu$ , and  $\tan\beta$ . Figure 11 shows the limit on the cross section for  $\tilde{\chi}_1^+\tilde{\chi}_1^-$  and  $\tilde{\chi}_1^\pm\tilde{\chi}_2^0$  production as a function of the  $\tilde{\chi}_1^\pm$  mass when  $|\mu|$  is large and thus the  $\tilde{\chi}_1^\pm$  mass is approximately twice the  $\tilde{\chi}_1^0$  mass. The figure also shows, more generally, the excluded region in the  $M_2$ - $\mu$  plane, along with a prediction for the region that might explain the CDF  $ee\gamma\gamma\cancel{E}_T$  event as  $\tilde{\chi}_1^+\tilde{\chi}_1^-$  production. The latter explanation requires  $100 \text{ GeV} < M_{\tilde{\chi}_1^\pm} < 150 \text{ GeV}$  with  $M_{\tilde{\chi}_1^0} < 0.6M_{\tilde{\chi}_1^\pm}$  to produce one event with a reasonable probability. As can be seen from Fig. 11, the cross section limit is typically 0.24 pb for either  $\tilde{\chi}_1^+\tilde{\chi}_1^-$  or  $\tilde{\chi}_1^\pm\tilde{\chi}_2^0$  production. By combining all  $\tilde{\chi}^\pm$  and  $\tilde{\chi}^0$  pair production processes, a  $\tilde{\chi}_1^\pm$  with mass below 150 GeV is excluded. Hence, to keep the  $\tilde{\chi}_1^+\tilde{\chi}_1^-$  interpretation of the  $ee\gamma\gamma\cancel{E}_T$  event, it would be necessary to expand the analysis of Ref. [68].

DØ also has a limit on the cross section for  $\tilde{e}\tilde{e}^* \rightarrow e^-e^+\tilde{\chi}_2^0\tilde{\chi}_2^0$ ,  $\tilde{\nu}\tilde{\nu}^* \rightarrow \nu\bar{\nu}\tilde{\chi}_2^0\tilde{\chi}_2^0$ , and  $\tilde{\chi}_2^0\tilde{\chi}_2^0 \rightarrow \gamma\gamma\tilde{\chi}_1^0\tilde{\chi}_1^0$  using the same analysis as for the  $\tilde{G}$  LSP search. Such signatures might also be expected in Higgsino LSP models. The limit on



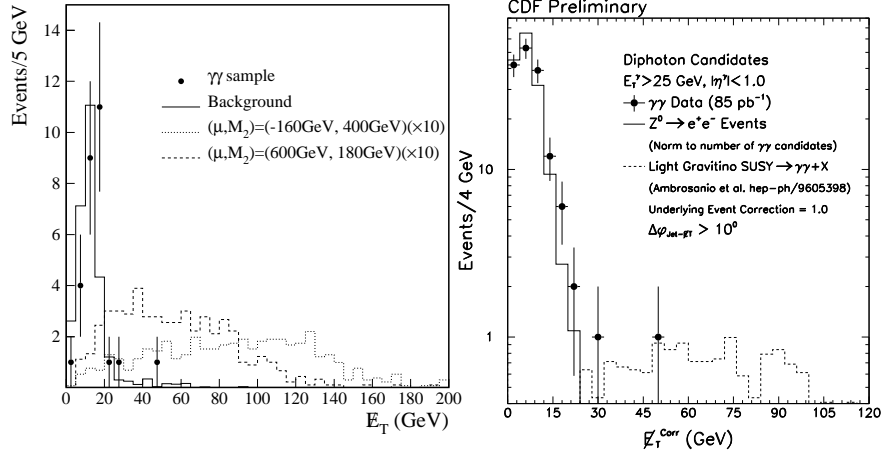


Figure 10: (Left) The  $E_T$  spectra in the  $D0$  search for events with 2  $\gamma$ 's, one with  $E_T > 20$  GeV, the other with  $E_T > 12$  GeV.<sup>75</sup> The points are the data, the solid line is the estimated background from di-jet events and direct  $\gamma$  events. The dotted lines are for gaugino production within gauge-mediated models using the parameters listed and  $M_1 \simeq 2M_2$ . (Right) The CDF  $E_T$  spectrum for events with two central  $\gamma$ 's with  $E_T > 25$  GeV. Events which have any jet with  $E_T > 10$  GeV pointing within 10 degrees in azimuth of the  $\cancel{E}_T$  are removed. The solid histogram shows the resolution from the  $Z \rightarrow e^+e^-$  control sample. The dashed line shows the expected distribution from all SUSY production in a model<sup>70</sup> with  $M_2 = 225$  GeV,  $\mu = 300$  GeV,  $\tan \beta = 1.5$ , and  $M_{\tilde{Q}} = 300$  GeV.

the cross section for such processes is about 0.35 pb for  $M_{\tilde{\chi}_2^0} - M_{\tilde{\chi}_1^0} > 30$  GeV, which is close to the maximum cross section predicted in these models.

CDF has searched for the signature  $\gamma b \cancel{E}_T$ , as predicted in Higgsino LSP models with a light  $\tilde{t}$ .<sup>73</sup> The data sample of 85 pb<sup>-1</sup> contains events with an isolated  $\gamma$  with  $E_T^\gamma > 25$  GeV and a jet with an SVX  $b$ -tag. After requiring  $\cancel{E}_T > 20$  GeV, 98 events remain.<sup>74</sup> The estimated background to the 98 events is  $77 \pm 23 \pm 20$  events. The shape is consistent with background. About 60% of the background is due to jets faking  $\gamma$ 's, 13% to real  $\gamma$ 's and fake  $b$ -tags, and the remainder to SM  $\gamma b \bar{b}$  and  $\gamma c \bar{c}$  production; all of these sources require fake  $\cancel{E}_T$ . When the  $\cancel{E}_T$  cut is increased to 40 GeV, 2 events remain. More than 6.4 events of anomalous production in this topology is excluded. The efficiency used in the limits is derived from a “baseline” model with  $M_{\tilde{\chi}_1^0} = 40$  GeV,  $M_{\tilde{\chi}_2^0} = 70$  GeV,  $m_{\tilde{t}_1} = 60$  GeV,  $m_{\tilde{Q}} = 250$  GeV, and  $M_{\tilde{g}} = 225$  GeV. The baseline model predicts 6.65 events, so this model is excluded (at the 95% C.L.). This result does not rule out the Higgsino LSP model with a light  $\tilde{t}$  in

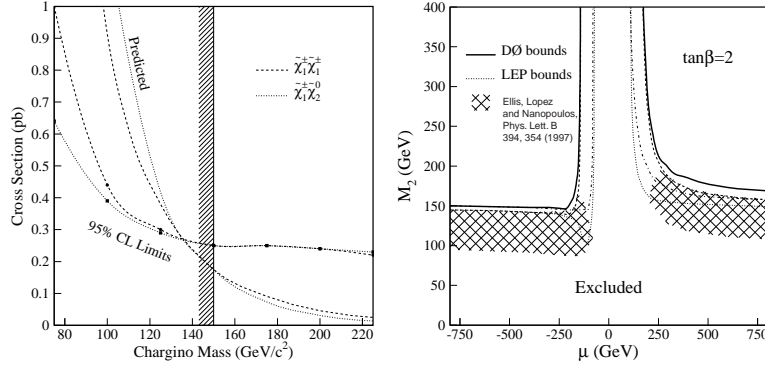


Figure 11: (Left) The DØ cross section limit on  $\tilde{\chi}_1^\pm \tilde{\chi}_1^\pm$  and  $\tilde{\chi}_1^\pm \tilde{\chi}_2^0$  production, assuming  $M_{\tilde{\chi}_1^\pm} \approx 2M_{\tilde{\chi}_1^0}$  and  $\text{BR}(\tilde{\chi}_1^0 \rightarrow \gamma \tilde{G}) = 100\%$ . The top dotted (dashed) curve is the cross section from PYTHIA for  $\tilde{\chi}_1^\pm \tilde{\chi}_2^0$  ( $\tilde{\chi}_1^+ \tilde{\chi}_1^-$ ) production. The bottom dotted (dashed) curve is the cross section limit from the DØ collaboration<sup>75</sup> on  $\tilde{\chi}_1^\pm \tilde{\chi}_2^0$  ( $\tilde{\chi}_1^+ \tilde{\chi}_1^-$ ) production. The vertical, hatched line marks the 95% C.L. lower limit on the lightest chargino mass from considering all chargino and neutralino pair production processes and all values of  $\mu$ . (Right) The limits on the parameters  $M_2$  and  $\mu$  in gauge-mediated models based on PYTHIA for  $\tan \beta = 2$  and  $M_{\tilde{Q}} = 800$  GeV.<sup>75</sup> The hatched area is the region proposed<sup>68</sup> to explain the CDF  $ee\gamma\gamma E_T$  event. The solid line shows the DØ bounds. The long-dashed line shows a contour with  $M_{\tilde{\chi}_1^\pm} = 150$  GeV and the dash-dotted line shows a contour with  $M_{\tilde{\chi}_1^0} = 75$  GeV. The dotted lines show an interpretation of preliminary LEP results at an energy of 161 GeV.

general, only one version with a fairly light mass spectrum. A more general limit can be set by holding the lighter sparticle masses constant and varying the  $\tilde{Q}$  and  $\tilde{g}$  masses. In this case  $\tilde{Q}$ 's and  $\tilde{g}$ 's less than 200 GeV and 225 GeV, respectively, are excluded.

#### 4 Conclusions

As can be seen from Table 1, there has been much effort directed into SUSY searches at the Tevatron. However, given the wide range of possible experimental signatures in the MSSM, there is still work in progress and much to be done. Many Run I analyses are under way.

In Run II, two upgraded detectors at the Tevatron will collect more data at a higher energy of 2 TeV. The nominal integrated luminosity is  $2 \text{ fb}^{-1}$ , with a possible extension to 10 or even  $30 \text{ fb}^{-1}$ . The production cross sections for heavy sparticles will increase significantly with the higher energy, and the

$\tilde{\chi}^\pm$  and  $\tilde{\chi}^0$  searches, as well as  $\tilde{Q}$  and  $\tilde{g}$  searches, will cover a wide range of SUSY parameter space. The experience gained from Run I analyses will greatly increase the quality of the Run II searches.<sup>76,77</sup> New triggering capabilities will open up previously inaccessible channels, particularly those involving  $\tau$ 's and heavy flavor. Increased  $b$ -tagging efficiency and  $\cancel{E}_T$  resolution will enhance many analyses. By extending Run II up to an integrated luminosity of about  $20 \text{ fb}^{-1}$  and combining search channels, the Tevatron can perform a crucial test of the MSSM Higgs boson sector. A factor of 20 or more data combined with improved detector capabilities makes the next Run at the Tevatron an exciting prospect.

### Acknowledgments

The authors thank G.L. Kane for suggesting this review, and the following people for useful discussions and comments: H. Baer, A. Beretvas, J. Berryhill, B. Bevensee, S. Blessing, A. Boehnlein, D. Chakraborty, P. Chankowski, M. Chertok, D. Claes, R. Demina, J. Done, E. Flattum, C. Grosso-Pilcher, J. Hobbs, M. Hohlmann, T. Kamon, S. Lammel, A. Lyon, D. Norman, M. Paterno, S. Pokorski, J. Qian, A. Savoy-Navarro, H.C. Shankar, M. Spira, D. Stuart, B. Tannenbaum, X. Tata, D. Toback, C. Wagner, N. Whiteman, P. Wilson and P. Zerwas.

### References

1. F. Abe, *et al.*, (CDF), Nucl. Instrum. Meth. **A271**, 387 (1988).
2. S. Abachi, *et al.*, (DØ), Nucl. Instrum. Meth. **A338**, 185 (1994), and references therein.
3. M. Carena, R.L. Culbertson, S. Eno, H.J. Frisch, and S. Mrenna, submitted to Rev. Mod. Phys., hep-ex/9712022.
4. Refs. [4–9] in Ref. [3], this chapter.
5. S. Dawson, E. Eichten and C. Quigg, Phys. Rev **D31**, 1581 (1985), and references on particular signatures given afterwards in this chapter.
6. M. Carena, J.R. Espinosa, M. Quirós and C.E.M. Wagner, Phys. Lett. **B335**, 209 (1995); M. Carena, M. Quirós and C.E.M. Wagner, Nucl. Phys. **B461**, 407 (1996); H. Haber, R. Hempfling and H. Hoang, Z. Phys. **75**, 539 (1997); M. Carena, P. Zerwas and the Higgs Physics Working Group, *Physics at LEP2*, Vol. 1, eds. G. Altarelli, T. Sjöstrand and F. Zwirner, CERN Report No. 96–01.
7. A. Stange, W. Marciano and S. Willenbrook, Phys. Rev. **D49** 1354 (1994) and Phys. Rev. **D50**, 4491 (1994); J. Dai J. Gunion and R,

- Vega, Phys. Rev. Lett **71**, 2699 (1993); Report of the TeV 2000 Study Group: Light Higgs Physics, FERMILAB-PUB-96/046; W.M. Yao, FERMILAB-CONF-96-383-E, 1996 Snowmass proceedings; S. Kim, S. Kuhlmann and W.M. Yao, 1996 Snowmass proceedings.
8. S. Mrenna and G.L. Kane, hep-ph/9406337; S. Mrenna, in *Perspectives on Higgs Physics*, edited by G.L. Kane (World Scientific, Singapore, 1997).
  9. S.P. Martin, this book; Refs. [15–19] in Ref. [3], this chapter.
  10. T. Sjöstrand, Comput. Phys. Commun. **82**, 74 (1994).  
S. Mrenna, Comput. Phys. Commun. **101**, 232 (1997).
  11. F. Paige and S.D. Protopopescu, *Supercollider Physics*, ed. D. Soper, 41 (World Scientific, 1986); H. Baer, F. Paige, S. Protopopescu and X. Tata, in *Proceedings of the Workshop on Physics at Current Accelerators* and Brookhaven National Laboratory report No. 38304, 1986 (unpublished).
  12. Ref. [20] in Ref. [3], this chapter.
  13. Refs. [17,22–26] in Ref. [3], this chapter.
  14. Refs. [26,28–30] in Ref. [3], this chapter.
  15. Ref. [31] in Ref. [3], this chapter.
  16. R. Barbieri and L. Maiani, Nucl. Phys. **B243**, 129 (1989).  
R. Barbieri, N. Cabbibo, L. Maiani and S. Petrarca, Phys. Lett. **B127**, 458 (1983).  
G.R. Farrar and A. Masiero, hep-ph/9410401.  
G.R. Farrar, hep-ph/9508291.
  17. Refs. [36,108–114] in Ref. [3], this chapter.
  18. Ref. [37] in Ref. [3], this chapter.
  19. Ref. [21] in Ref. [3], this chapter.
  20. H. Dreiner, An introduction to Explicit R-parity Violation, to be published in *Perspectives on Supersymmetry*, ed. G.L. Kane, (World Scientific, Singapore, 1997), hep-ph 9707435 and references therein; G. Bhattacharyya, A Brief Review on R-Parity-Violating couplings, invited talk at Beyond the Desert, Castle Ringberg, Tengenrsee, Germany, June 1997, hep-ph/9709395.
  21. Refs. [54,56–58] in Ref. [3], this chapter.
  22. F. Abe, *et al.*, (CDF), Phys. Rev. Lett. **76**, 4307 (1996).
  23. B. Bevensee, (CDF), *Proceedings of The International Workshop on Quantum Effects in the MSSM*, (Barcelona, Spain, 1997), FERMILAB-CONF-97/405-E.
  24. S. Abachi, *et al.*, (DØ), Phys. Rev. Lett. **76**, 2228 (1996).
  25. B. Abbott, *et al.*, (DØ), submitted to Phys. Rev. Lett., FERMILAB PUB-97/201-E, hep-ex/9705015.

26. H. Baer and X. Tata, Phys. Rev. **D47**, 2739 (1993).
27. S. Mrenna, G.L. Kane, G.D. Kribs and J.D. Wells, Phys. Rev. **D53**, 1168 (1996).
28. W. Beenakker, R. Hopker, M. Spira and P.M. Zerwas, Z. Phys. **C69**, 163 (1995), Phys. Rev. Lett. **74** 2905 (1995), and Nucl. Phys. **B492**, 51 (1997); W. Beenakker, R. Hopker, and M. Spira, hep-ph/9611232; W. Beenakker, M. Kramer, T. Plehn, M. Spira and P.M. Zerwas, hep-ph/9710451.
29. H. Baer, X. Tata and J. Woodside, Phys. Rev. Lett. **63**, 352 (1989). Phys. Rev. **D41**, 906 (1990), and Phys. Rev. **D44**, 207 (1991).
30. V. Barger, Y. Keung and R.J. Philips, Phys. Rev. Lett. **55**, 166 (1985). R.M. Barnett, J. Gunion and H. Haber, Phys. Lett. **B315**, 349 (1993). H. Baer, C. Kao and X. Tata, Phys. Rev. **D48**, 2978 (1993).
31. S. Abachi *et al.*, (DØ), Phys. Rev. Lett. **75**, 618 (1995).
32. S. Abachi *et al.*, (DØ), FERMILAB-CONF-97/357-E.
33. F.A. Berends, H. Kuijf, B. Tausk and W.T. Giele, Nucl. Phys. **B357**, 32 (1991).
34. G. Marchesini and B. R. Webber, Nucl. Phys. **B238**, 1 (1984) and Nucl. Phys. **B310**, 461 (1988).
35. F. Abe, *et al.*, (CDF), Phys. Rev. **D56**, 1357 (1997).
36. S. Abachi, *et al.*, (DØ), *Proceedings of the 28<sup>th</sup> International Conference on High Energy Physics*, eds. Z. Ajduk and A. K. Wroblewski (World Scientific, Singapore, 1997), FERMILAB-CONF-96/427-E.
37. F. Abe, *et al.*, (CDF), Phys. Rev. Lett. **76**, 2006 (1996).
38. J. Done, (CDF), *Proceedings of 1996 Divisional Meeting of the Division of Particles and Fields*, (DPF '96 Minneapolis, MN, 1996), FERMILAB-CONF-96/371-E.
39. H. Baer, M. Drees, R. Godbole, J. Gunion and X. Tata, Phys. Rev. **D44**, 725 (1991).
40. H. Baer, J. Sender and X. Tata, Phys. Rev. **D50**, 4517 (1994).
41. S. Abachi, *et al.*, (DØ), Phys. Rev. Lett. **76**, 2222 (1996).
42. P. Azzi, (CDF), *Proceedings of XXXII Rencontres de Moriond, QCD and High Energy Hadronic Interactions*, Les Arcs, France, 1997, FERMILAB-CONF-97/148-E (to be published).
43. S. Abachi, *et al.*, (DØ), FERMILAB-PUB-96/449-E, hep-ex/9612009.
44. P.J. Wilson, (CDF), *Proceedings of Les Rencontres de Physique de La Vallee D'Aosta*, La Thuile, Italy, 1997, FERMILAB-CONF-97-241-E (to be published).
45. H. Baer, C. Chen, F. Paige and X. Tata, Phys. Rev. **D49**, 3283 (1994).
46. R.M. Godbole and D.P. Roy, Phys. Rev. **D43**, 3640 (1991).

- M. Guchait and D.P. Roy, Phys. Rev. **D55**, 7263 (1997).
47. F. Abe, *et al.*, (CDF), Phys. Rev. Lett. **72**, 1977 (1994); see also C. Jessop, Ph.D thesis, Harvard University, 1994. This analysis uses  $4.2 \text{ pb}^{-1}$  from the 1989 run and a signature of a hadronically-decaying  $\tau + \geq 1 \text{ jet} + \cancel{E}_T$ .
  48. F. Abe, *et al.*, (CDF), Phys. Rev. **D54**, 357 (1997).
  49. S. Abachi, *et al.*, (DØ), FERMILAB-CONF-97/386-E.
  50. J. Gausch, R. Jimenez and J. Sola, Phys. Lett. **B360**, 47 (1995); J. Coarasa, D. Garcia, J. Guasch, R. Jimenez, J. Sola, to appear in Z. Phys. **C**; J. Guasch and J. Sola, to appear in Phys. Lett. **B**, hep-ph/9707535; J. Sola, hep-ph/9708494.
  51. J. Dai, J. F. Gunion and R. Vega, Phys. Lett. **B387** 801 (1996).
  52. S. Abachi, *et al.*, (DØ), *Proceedings of the 28<sup>th</sup> International Conference on High Energy Physics*, eds. Z. Ajduk and A. K. Wroblewski (World Scientific, Singapore, 1997), FERMILAB-CONF-96/427-E.
  53. F. Abe, *et al.*, (CDF), submitted to Phys. Rev. Lett., FERMILAB-PUB-97-247-E.
  54. J. A. Valls, (CDF), *Proceedings 32nd Rencontres de Moriond*, Les Arcs, France, March, 1997, FERMILAB-CONF-97/135-E.
  55. S. Abachi, *et al.*, (DØ), FERMILAB-CONF-97/325-E.
  56. F. Abe, *et al.*, (CDF), Phys. Rev. **D54**, 735 (1996). This analysis uses  $18.7 \text{ pb}^{-1}$  from Run Ia and a signature of a hadronically-decaying  $\tau + \geq 1 \text{ jet} + \cancel{E}_T$ .
  57. F. Abe, *et al.*, (CDF), Phys. Rev. Lett. **73**, 2667 (1994); J. Wang, Ph.D thesis, University of Chicago, 1994. This analysis uses  $19.3 \text{ pb}^{-1}$  from Run Ia and a signature of two leptons +  $\cancel{E}_T$ .
  58. S. Abachi, *et al.*, (DØ), FERMILAB-CONF-97/325-E.
  59. K. Maeshima, (CDF), *Proceedings of the 28th International Conference on High Energy Physics*, eds. Z. Ajduk and A. K. Wroblewski (World Scientific, Singapore, 1997), FERMILAB-CONF-96-412-E.
  60. Ref. [103] in Ref. [3], this chapter.
  61. X. Wu, (CDF), talk at International Europhysics Conference on High Energy Physics, Jerusalem, Israel, 1997.
  62. D. Choudhury and S. Raychaudhuri, Phys. Rev. **D56**, 1778 (1997).
  63. S. Park, (CDF), *Proceedings of the 10th Topical Workshop on Proton-Antiproton Collider Physics*, eds. R. Raja and J. Yoh, (AIP Press, Woodbury, NY, 1996).
  64. G. Bhattacharyya and R.N. Mohapatra, Phys. Rev. **D54**, 4204 (1996). J. L. Rosner, Phys. Rev. **D55**, 3143 (1997).
  65. S. Dimopoulos, M. Dine, S. Raby and S. Thomas, Phys. Rev. Lett. **76**,

- 3494 (1996) and Phys. Rev. **D55**, 1372 (1997).
66. S. Ambrosanio, G.L. Kane, G.D. Kribs, S.P. Martin and S. Mrenna, Phys. Rev. Lett. **76**, 3498 (1996).
  67. S. Dimopoulos, S. Thomas and J. Wells, Phys. Rev. **D54**, 3283 (1996) and Nucl. Phys. **B488**, 39 (1997).  
S. Dimopoulos, M. Dine, S. Raby, S. Thomas and J. Wells, Nucl. Phys. Proc. Suppl. **A52**, 38 (1997).  
D. Dicus, B. Dutta and S. Nandi, Phys. Rev. Lett. **78**, 3055 (1997) and Phys. Rev. **D56**, 5748 (1997).
  68. J. Ellis, J.L. Lopez and D.V. Nanopoulos, Phys. Lett. **B394**, 354 (1997).
  69. P. Fayet, Phys. Lett. **B70**, 461 (1977); P. Fayet, Phys. Lett. **B84**, 416 (1979); R. Casalbuoni, S. de Curtis, D. Dominici, F. Feruglio and R. Gatto, Phys. Lett. **B215**, 313 (1988).
  70. S. Ambrosanio, G.L. Kane, G.D. Kribs, S.P. Martin and S. Mrenna, Phys. Rev. **D54**, 5395 (1996).
  71. H. Baer, M. Brhlik, C-H. Chen and X. Tata, Phys. Rev. **D55**, 4463 (1997).
  72. H.E. Haber, G.L. Kane and M. Quiros, Phys. Lett. **B160**, 297 (1985) and Nucl. Phys. **B273**, 333 (1986).
  73. S. Mrenna and G.L. Kane, Phys. Rev. Lett. **77**, 3502 (1996).
  74. R.L. Culbertson, (CDF and DØ), to be published in Nucl. Phys. **B**, *Proceedings of the 5th International Conference on Supersymmetries in Physics* (SUSY '97), Philadelphia, PA, 1997, FERMILAB-CONF-97-277-E.
  75. S. Abachi, *et al.*, (DØ), submitted to Phys. Rev. Lett., FERMILAB-PUB-97/273-E.
  76. D. Amidei, *et al.*, *Future Electroweak Physics at the Fermilab Tevatron: Report of the TeV-2000 Study Group*, FERMILAB-PUB-96-082.
  77. J. Amundson, *et al.*, *Report of the Supersymmetry Theory Subgroup in New Directions for High-Energy Physics*, eds. D. Cassel, L. Gennari and R. Siemann, 644 (SLAC, Stanford, 1997).